POSTBUCKLING BEHAVIOR OF RECTANGULAR PLATES

by

Manuel Stein, B.S.M.E., M.A.E.

Dissertation submitted to the Graduate Faculty of the

Virginia Polytechnic Institute

in candidacy for the degree of

DOCTOR OF PHILOSOPHY

in

Applied Mechanics

APPROVED:

_____

Chairman, Advisory Committee

_____ _____

_____

June 1958

Blacksburg, Virginia

II. TABLE OF CONTENTS

PAGE

III. LIST OF TABLES AND FIGURES

IV. SYMBOLS

a	plate length
b	plate width
h	plate thickness
i,j,m,n,r,s	integers
l	length of each of the three rigid rods in column
u, v	displacement of point on middle surface of plate in x and y directions, respectively
w	deflection of point on middle surface of plate in direction normal to undeformed plate
x, y	plate coordinates
C	stiffness of torsional springs
D	plate flexural stiffness, $D = \frac{Eh^3}{12(1 - \mu^2)}$
E	Young's modulus for material
K, K_1	stiffness of nonlinear extensional springs, units are force/(length)^3
P	total compressive load
T	temperature rise
w_1, w_2	deflection of joints in column
N_x, N_y	resultant normal forces in x and y directions, respectively
N_{xy}	resultant shearing force in xy plane
P_{cr}	buckling load
T_{cr}	temperature rise for buckling

α coefficient of thermal expansion

β buckle length-width ratio, $\beta = mb/a$

ϵ arbitrary parameter

ξ, η functions of deflection, $\xi = \frac{w_1 + w_2}{2}$, $\eta = \frac{w_1 - w_2}{2}$

μ Poisson's ratio for material

Δ total shortening (see eqs. (28) or (34))

γ_{xy} middle surface shearing strain

ϵ_x, ϵ_y middle surface strains in x and y directions

ϵ_{x_b} bending strain at crest of buckle

ϵ_{x_o} extreme fiber strain at crest of buckle

$$\nabla^4 = \frac{\partial^4}{\partial x^4} + 2\frac{\partial^4}{\partial x^2 \partial y^2} + \frac{\partial^4}{\partial y^4}$$

V. INTRODUCTION

In the design of aircraft structural components, it is important to know the load-carrying capacity of rectangular flat plates and their behavior when subject to change in temperature. Under extreme conditions these rectangular plates may buckle; that is, the forces in the middle plane of the plate increase up to values for which the flat form of equilibrium becomes unstable. Unlike simple columns, rectangular plates which are supported on all edges may carry considerable load beyond their buckling load. Under some conditions it may be advantageous to utilize this additional load-carrying capacity. Very often the load required for buckling is in the elastic range for the plate material and part of the postbuckling range is elastic. Even if this were not true, it is necessary to understand the behavior in the elastic range before considering the case where the material may yield in the plastic range. This dissertation studies the postbuckling behavior of simply supported rectangular flat plates in the elastic range of the material. The use of a simply supported edge condition should provide a conservative estimate of the postbuckling behavior of a rectangular plate contained between the relatively stiff supporting elements (stringers, ribs) of thin wall construction.

Many authors have studied the postbuckling behavior of flat rectangular plates; some of the most important of these investigations are described in references 1 to 13. The basic differential equations for a plate element undergoing large deflections are presented by von Karman.[1]

Von Karman, Sechler, and Donnell[2] introduce the concept of effective width. Various approximate solutions for postbuckling behavior are presented by Cox,[3] Timoshenko,[4] Marguerre and Trefftz,[5] and Marguerre,[6] where analyses are carried out by energy methods. Kromm and Marguerre[7] extend the results of references 5 and 6 for simply supported infinitely long plates in compression. By means of Fourier series, Levy[8] obtained an exact solution to the large deflection equations of von Karman[1] for square plates. Koiter[9] extends the work of reference 7 to make it applicable far beyond buckling. The effects of initial deviation from flatness for square plates are investigated by Hu, Lundquist, and Batdorf[10] and by Coan[11] by means of the Fourier series method of solution advanced in reference 8. In reference 10, the unloaded edges of the plate are constrained to remain straight, whereas in reference 11, the side edges are free to distort in the plane of the plate. Mayers and Budiansky[12] analyze the behavior of a square plate compressed beyond the elastic buckling load into the range where plastic yielding takes place. Alexeev[13] obtained an exact solution for the square plate buckling into one buckle as did Levy but included in addition an exact solution for the square plate buckling into two buckles (in the direction of loading).

With the exception of reference 13, all of the previous authors studying the postbuckling behavior of rectangular plates used either energy methods or Fourier-series expansion of the basic nonlinear differential equations of von Karman. Alexeev[13] used a method of successive approximation. In this dissertation the basic nonlinear differential

equations are converted into an infinite set of linear differential equations by expanding the displacements into a power series in terms of an arbitrary parameter. The first few of the equations of the infinite set turn out to be the small deflection equations. Solution of these and succeeding equations permits a study of the behavior of the plate at buckling and beyond, up into the large deflection range. The postbuckling behavior of a simply supported plate subjected to longitudinal compression is studied in detail, and the results are compared to other theoretical results. A similar study is presented for such a plate subject to a uniform temperature rise.

The method of solution presented here for plate problems is similar to a perturbation method. However, in a perturbation method consideration is restricted to solutions which involve only small values of the arbitrary parameter. For the case investigated in detail here and for some similar cases investigated, it is not necessary to restrict the arbitrary parameter to small values because the coefficients of the higher powers are small. The motivation for this work was the observation that available solutions of the postbuckling behavior of rectangular plates subject to longitudinal compression indicated that both the shortening and the square of the center deflection were nearly linear functions of the applied load in the first part of the postbuckling range. For the compression problem it was thus expected that the first few terms of a series in powers of $(P - P_{cr})/P_{cr}$ would be adequate to represent the displacements. (P is the total applied load and P_{cr} is the critical load.) These expectations have been borne out.

One of the phenomena which occurs in the postbuckling range is change in buckle pattern. Because of the incompleteness and the inconsistancies in the treatment of this topic in the literature[7,9,13,14,15] a study is made in this dissertation of change in buckle pattern. In order to analyze this phenomenon in a rigorous fashion a symmetric three-element column on a nonlinear elastic foundation is solved. It is indicated how the principles learned from the column analysis may be applied qualitatively to plate problems.

Experimental results which have not been published previously are described in this dissertation and results from these and other experiments are compared with the present theory.

VI. THEORY

In this section the von Karman large deflection plate equations will be converted from a set of three nonlinear partial differential equations into an infinite set of linear partial differential equations by expanding the displacements into a power series in terms of an arbitrary parameter.

For a plate with no lateral load the von Karman large deflection equations can be written in the form

$$N_{x,x} + N_{xy,y} = 0 \tag{1a}$$

$$N_{y,y} + N_{xy,x} = 0 \tag{1b}$$

$$D\nabla^4 w - (N_x w_{,xx} + N_y w_{,yy} + 2N_{xy} w_{,xy}) = 0 \tag{1c}$$

where subscripts x and y which appear after a comma indicate partial differentiation with respect to x and y, respectively. The strain-stress relations including the effects of change in temperature T are

$$\epsilon_x = \frac{1}{Eh}(N_x - \mu N_y) + \alpha T \tag{2a}$$

$$\epsilon_y = \frac{1}{Eh}(N_y - \mu N_x) + \alpha T \tag{2b}$$

$$\gamma_{xy} = \frac{2(1 + \mu)}{Eh} N_{xy} \tag{2c}$$

or the stresses appearing in equation (2) may be solved for and thus expressed in terms of the strains.

$$N_x = \frac{Eh}{1 - \mu^2}\left[(\epsilon_x + \mu\epsilon_y) - (1 + \mu)\alpha T\right] \tag{3a}$$

$$N_y = \frac{Eh}{1 - \mu^2}\left[(\epsilon_y + \mu\epsilon_x) - (1 + \mu)\alpha T\right] \tag{3b}$$

$$N_{xy} = \frac{Eh}{2(1 + \mu)}\gamma_{xy} \tag{3c}$$

The strain-displacement relations are

$$\epsilon_x = u_{,x} + \frac{1}{2}w_{,x}^2 \tag{4a}$$

$$\epsilon_y = v_{,y} + \frac{1}{2}w_{,y}^2 \tag{4b}$$

$$\gamma_{xy} = u_{,y} + v_{,x} + w_{,x}w_{,y} \tag{4c}$$

Equations (1), (3), and (4), together with a complete set of boundary conditions, determine the problem. These equations are subject to the usual out-of-plane (zero normal deflection and zero moment for simply supported plates) boundary conditions required in buckling studies. In addition, however, for postbuckling studies it is necessary to specify in-plane conditions. Note that only plates without initial eccentricities subject to in-plane loading are considered.

It is assumed that u, v, and w may be expanded in a power series in terms of an arbitrary parameter ϵ. For the present purposes u, v, and w are to be expanded about the point of buckling (at buckling $\epsilon = 0$).

$$u = \sum_{n=0,2}^{\infty} u^{(n)}\epsilon^n \tag{5a}$$

$$v = \sum_{n=0,2}^{\infty} v^{(n)}\epsilon^n \tag{5b}$$

$$w = \sum_{n=1,3}^{\infty} w^{(n)} \epsilon^n \tag{5c}$$

The $u^{(n)}$, $v^{(n)}$, and $w^{(n)}$ are functions of x and y only. For plates without initial eccentricities subject to in-plane loading the deflection w is zero in the loading range prior to buckling but u and v have values other than zero. Thus, for small values of ϵ, u and v would have values close to their values just prior to buckling while w may be proportional to ϵ or some power of ϵ. Therefore it is to be expected that series for u and v will start with the zero power of ϵ while the series for w will start with a nonzero power. As discussed in the introduction available solutions of the postbuckling behavior of rectangular plates subject to longitudinal compression indicated that the square of the center deflection was nearly a linear function of the applied load in the first part of the postbuckling range. Thus if ϵ is related to the load P so that $\epsilon^2 = (P - P_{cr})/P_{cr}$ for this compression problem the series for w would start with the first power.

For other problems the parameter ϵ may take on other character. For example, ϵ may be the lateral deflection of a reference point on the plate, or ϵ^2 may be the shortening or the average temperature rise beyond that required for buckling. The choice of ϵ should become evident in the solution of a problem.

As written, the series for u and v start with a zero power and include only even powers and the series for w starts with the first power and includes only odd powers. It will be indicated later

that for plates without initial eccentricities subject to any in-plane loading, the odd powers in the series for u and v and the even powers in the series for w will vanish, and, for simplicity, they have been omitted from the start. Incidently, it is possible to deduce that the odd powers in the series for u and v and the even powers in the series for w vanish once it is seen that the parameter ϵ may be plus or minus for a given load. For the type of problem considered the plate can buckle in either direction but the deflection shape $w(x,y)$ will be independent of the direction of buckling (except for a sign) anywhere in the postbuckling range. Hence, in order to provide that the shape will be independent of the direction of buckling the series for w can contain only odd powers of ϵ. The in-plane displacements u and v on the other hand are unchanged by the direction of buckling and, therefore, should include only even powers of ϵ. The change in temperature T also should include only even powers of ϵ:

$$T = \sum_{n=0,2}^{\infty} T^{(n)} \epsilon^n \tag{6}$$

where $T^{(n)}$ may be a function of x and y.

Upon substitution of the above equations (5) and (6) into equations (3) and (4), the following relations are obtained:

$$N_x = \sum_{n=0,2}^{\infty} N_x^{(n)} \epsilon^n + \sum_{m=1,3}^{\infty} \sum_{n=1,3}^{\infty} N_x^{(mn)} \epsilon^{m+n} \tag{7a}$$

$$N_y = \sum_{n=0,2}^{\infty} N_y^{(n)} \epsilon^n + \sum_{m=1,3}^{\infty} \sum_{n=1,3}^{\infty} N_y^{(mn)} \epsilon^{m+n} \tag{7b}$$

$$N_{xy} = \sum_{n=0,2}^{\infty} N_{xy}^{(n)} \epsilon^n + \sum_{m=1,3}^{\infty} \sum_{n=1,3}^{\infty} N_{xy}^{(mn)} \epsilon^{m+n} \tag{7c}$$

where

$$N_x^{(n)} = \frac{Eh}{1-\mu^2}\left[u_{,x}^{(n)} + \mu v_{,y}^{(n)} - (1+\mu)\alpha T^{(n)}\right]$$

$$N_y^{(n)} = \frac{Eh}{1-\mu^2}\left[v_{,y}^{(n)} + \mu u_{,x}^{(n)} - (1+\mu)\alpha T^{(n)}\right]$$

$$N_{xy}^{(n)} = \frac{Eh}{2(1+\mu)}\left(u_{,y}^{(n)} + v_{,x}^{(n)}\right)$$

$$N_x^{(mn)} = \frac{Eh}{2(1-\mu^2)}\left(w_{,x}^{(m)} w_{,x}^{(n)} + \mu w_{,y}^{(m)} w_{,y}^{(n)}\right) = N_x^{(nm)}$$

$$N_y^{(mn)} = \frac{Eh}{2(1-\mu^2)}\left(w_{,y}^{(m)} w_{,y}^{(n)} + \mu w_{,x}^{(m)} w_{,x}^{(n)}\right) = N_y^{(nm)}$$

$$N_{xy}^{(mn)} = \frac{Eh}{2(1+\mu)} w_{,x}^{(m)} w_{,y}^{(n)}$$

Since ϵ was taken to be an arbitrary parameter, the stipulation that a power series in ϵ vanishes requires that each coefficient of the power series vanishes. If the expressions (5c) and (7) for w and the N's are substituted in equations (1), the requirement that each coefficient in the power series vanishes leads to the following linear equations which are the first few of an infinite set

$$\left.\begin{aligned} N_{x,x}^{(0)} + N_{xy,y}^{(0)} &= 0 \\ N_{y,y}^{(0)} + N_{xy,x}^{(0)} &= 0 \end{aligned}\right\} \tag{8a}$$

$$D\nabla^4 w^{(1)} - \left(N_x^{(0)} w_{,xx}^{(1)} + N_y^{(0)} w_{,yy}^{(1)} + 2N_{xy}^{(0)} w_{,xy}^{(1)}\right) = 0 \tag{8b}$$

$$\left.\begin{aligned} N_{x,x}^{(2)} + N_{xy,y}^{(2)} &= -\left(N_{x,x}^{(11)} + N_{xy,y}^{(11)}\right) \\ N_{y,y}^{(2)} + N_{xy,x}^{(2)} &= -\left(N_{y,y}^{(11)} + N_{xy,x}^{(11)}\right) \end{aligned}\right\} \tag{8c}$$

$$D\nabla^4 w^{(3)} - \left(N_x^{(0)} w_{,xx}^{(3)} + N_y^{(0)} w_{,yy}^{(3)} + 2N_{xy}^{(0)} w_{,xy}^{(3)}\right) =$$

$$\left(N_x^{(2)} + N_x^{(11)}\right) w_{,xx}^{(1)} + \left(N_y^{(2)} + N_y^{(11)}\right) w_{,yy}^{(1)} + 2\left(N_{xy}^{(2)} + N_{xy}^{(11)}\right) w_{,xy}^{(1)} \tag{8d}$$

$$\left.\begin{aligned} N_{x,x}^{(4)} + N_{xy,y}^{(4)} &= -\left(2N_{x,x}^{(13)} + N_{xy,y}^{(13)} + N_{xy,y}^{(31)}\right) \\ N_{y,y}^{(4)} + N_{xy,x}^{(4)} &= -\left(2N_{y,y}^{(13)} + N_{xy,x}^{(13)} + N_{xy,x}^{(31)}\right) \end{aligned}\right\} \tag{8e}$$

$$D\nabla^4 w^{(5)} - \left(N_x^{(0)} w_{,xx}^{(5)} + N_y^{(0)} w_{,yy}^{(5)} + 2N_{xy}^{(0)} w_{,xy}^{(5)}\right) =$$

$$\left(N_x^{(2)} + N_x^{(11)}\right) w_{,xx}^{(3)} + \left(N_y^{(2)} + N_y^{(11)}\right) w_{,yy}^{(3)} + 2\left(N_{xy}^{(2)} + N_{xy}^{(11)}\right) w_{,xy}^{(3)} +$$

$$\left(N_x^{(4)} + 2N_x^{(13)}\right) w_{,xx}^{(1)} + \left(N_y^{(4)} + 2N_y^{(13)}\right) w_{,yy}^{(1)} +$$

$$2\left(N_{xy}^{(4)} + N_{xy}^{(13)} + N_{xy}^{(31)}\right) w_{,xy}^{(1)} \tag{8f}$$

etc.

It might be noted here that if the odd powers in the series for u and v and the even powers in the series for w had been included, they would have formed a set of homogeneous differential equations with homogeneous boundary conditions (which would not have coupled with the terms originally included) and therefore would have vanished.

Looking now at equations (8) above, it is seen that equation (8a) and (8b) can be identified as the usual (linear) small deflection equations. Solution of these and then some of the succeeding equations permits a study of the behavior of the plate at buckling and then beyond into the large deflection range (provided the series behave properly). At present the only ways available to determine convergence are by a comparison of the results obtained from the various approximations and by comparisons with other methods and with experiment.

VII. EXAMPLE COMPRESSION PROBLEM

Solution of the equations just derived in the previous section for a postbuckling problem of rectangular simply supported plates in compression is presented in this section. The origin of coordinates is taken at the corner of the plate which has the dimensions a and b as shown and which has the thickness h

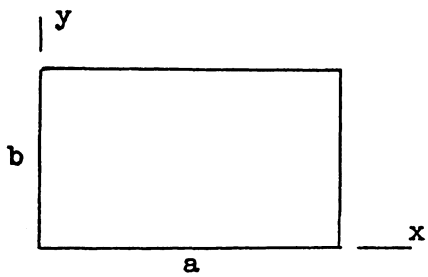

A. Solution

The problem solved is the postbuckling behavior of a rectangular simply supported plate in longitudinal compression with edges constrained so that the displacement of each edge in the plane of the plate is uniform. As discussed in the introduction, the simply supported edge condition is practical; with the in-plane conditions chosen here, it also leads to much simpler results than other kinds of edge support. For other types of edge support there is no conceptual difference in the method of solution.

The boundary conditions considered can be written

zero deflection $\quad w(o,y) = w(a,y) = w(x,o) = w(x,b) = 0$

zero moment $\quad w_{,xx}(o,y) = w_{,xx}(a,y) = w_{,yy}(x,o) = w_{,yy}(x,b) = 0$

constant displacement $\quad u_{,y}(o,y) = u_{,y}(a,y) = v_{,x}(x,o) = v_{,x}(x,b) = 0$

zero shear stress $\quad v_{,x}(o,y) = v_{,x}(a,y) = u_{,y}(x,o) = u_{,y}(x,b) = 0$

loaded edges $\quad \int_o^b (N_x)_{x=o,a}\, dy = -P$

unloaded edges $\quad \int_o^a (N_y)_{y=o,b}\, dx = 0$

Here P is the given total applied load and is equal to or above the buckling load. If for u, v, and w expressions (5) are inserted in the first four lines of boundary conditions, it is seen that the $u^{(n)}$, $v^{(n)}$, $w^{(n)}$ must individually satisfy these boundary conditions. Substituting from equation (7a) into the condition on the loaded edges gives

$$P = \sum_{n=0,2}^{\infty} P^{(n)} \epsilon^n \tag{9}$$

where

$$P^{(0)} = -\int_o^b \left(N_x^{(0)}\right)_{x=o,a} dy$$

$$P^{(2)} = -\int_o^b \left(N_x^{(2)} + N_x^{(11)}\right)_{x=o,a} dy \tag{10}$$

$$P^{(4)} = -\int_o^b \left(N_x^{(4)} + 2N_x^{(13)}\right)_{x=o,a} dy$$

etc.

Similarly, by using equation (7b), the condition on the unloaded edges becomes

$$\int_o^a \left(N_y^{(0)}\right)_{y=o,b} dx = 0$$

$$\int_o^a \left(N_y^{(2)} + N_y^{(11)}\right)_{y=o,b} dx = 0 \qquad (11)$$

$$\int_o^a \left(N_y^{(4)} + 2N_y^{(13)}\right)_{y=o,b} dx = 0$$

etc.

For this case there is no temperature rise; so all the $T^{(n)}$ are set equal to zero.

Solutions of equation (8a) for $u^{(0)}$ and $v^{(0)}$ that satisfy the boundary conditions are

$$\left.\begin{aligned} u^{(0)} &= -\frac{P^{(0)}}{Ehb}\left(x - \frac{a}{2}\right) \\ v^{(0)} &= \frac{\mu P^{(0)}}{Ehb}\left(y - \frac{b}{2}\right) \end{aligned}\right\} \qquad (12)$$

It therefore follows that

$$\left.\begin{aligned} N_x^{(0)} &= -\frac{P^{(0)}}{b} \\ N_y^{(0)} &= N_{xy}^{(0)} = 0 \end{aligned}\right\} \qquad (13)$$

Now $w^{(1)}$ can be determined from equation (8b) which has the solution

$$w^{(1)} = w_1 \sin\frac{m\pi x}{a} \sin\frac{n\pi y}{b} \qquad (14)$$

that satisfies the boundary conditions. This solution requires that

$$P^{(0)} = \frac{Db\left[\left(\frac{m\pi}{a}\right)^2 + \left(\frac{n\pi}{b}\right)^2\right]^2}{\left(\frac{m\pi}{a}\right)^2} \tag{15}$$

So far, the solutions obtained are identical to the small deflection solution where the set of the various values of $P^{(0)}$ (for each, m,n combination) can be identified as the set of buckling loads. The lowest buckling load is determined by the choice of m and n for a particular length-width ratio a/b. Note that, as in small deflection theory, the amplitude w_1, cannot be determined (as yet).

The $N^{(11)}$'s may now be found (in terms of w_1) and from equations (8c) solutions that satisfy the boundary conditions are

$$\left.\begin{aligned} u^{(2)} &= -\left[\frac{P^{(2)}}{Ehb} + \frac{w_1^2}{8}\left(\frac{m\pi}{a}\right)^2\right]\left(x - \frac{a}{2}\right) - \frac{w_1^2}{16}\left[\frac{\left(\frac{m\pi}{a}\right)^2 - \mu\left(\frac{n\pi}{b}\right)^2}{\frac{m\pi}{a}} \sin\frac{2m\pi x}{a} - \right. \\ &\qquad \left. \frac{m\pi}{a} \sin\frac{2m\pi x}{a} \cos\frac{2n\pi y}{b}\right] \\ v^{(2)} &= \left[\frac{\mu P^{(2)}}{Ehb} - \frac{w_1^2}{8}\left(\frac{n\pi}{b}\right)^2\right]\left(y - \frac{b}{2}\right) - \frac{w_1^2}{16}\left[\frac{\left(\frac{n\pi}{b}\right)^2 - \mu\left(\frac{m\pi}{a}\right)^2}{\frac{n\pi}{b}} \sin\frac{2n\pi y}{b} - \right. \\ &\qquad \left. \frac{n\pi}{b} \cos\frac{2m\pi x}{a} \sin\frac{2n\pi y}{b}\right] \end{aligned}\right\} \tag{16}$$

so that

$$\left.\begin{aligned} N_x^{(2)} + N_x^{(11)} &= -\frac{P^{(2)}}{b} - \frac{Ehw_1^2}{8}\left(\frac{m\pi}{a}\right)^2 \cos\frac{2n\pi y}{b} \\ N_y^{(2)} + N_y^{(11)} &= -\frac{Ehw_1^2}{8}\left(\frac{n\pi}{b}\right)^2 \cos\frac{2m\pi x}{a} \\ N_{xy}^{(2)} + N_{xy}^{(11)} &= 0 \end{aligned}\right\} \qquad (17)$$

Now $w^{(3)}$ must be determined from equation (8d). After substitution of the N's and $w^{(1)}$, equation (8d) becomes

$$D\nabla^4 w^{(3)} + \frac{P^{(0)}}{b} w^{(3)}_{,xx} = w_1\left(\left\{\frac{P^{(2)}}{b}\left(\frac{m\pi}{a}\right)^2 - \frac{Ehw_1^2}{16}\left[\left(\frac{m\pi}{a}\right)^4 + \left(\frac{n\pi}{b}\right)^4\right]\right\}\sin\frac{m\pi x}{a}\sin\frac{n\pi y}{b} + \frac{Ehw_1^2}{16}\left(\frac{m\pi}{a}\right)^4 \sin\frac{m\pi x}{a}\sin\frac{3n\pi y}{b} + \frac{Ehw_1^2}{16}\left(\frac{n\pi}{b}\right)^4 \sin\frac{3m\pi x}{a}\sin\frac{n\pi y}{b}\right) \qquad (18)$$

It should be noted that $\sin\frac{m\pi x}{a}\sin\frac{n\pi y}{b}$ is a homogeneous solution to equation (18), and that since a term of this kind appears on the right hand side of this equation special methods must be used to get a particular solution. In fact, no solution to equation (18) is possible that satisfies boundary conditions of this problem unless the coefficient of the $\sin\frac{m\pi x}{a}\sin\frac{n\pi y}{b}$ term on the right hand side of this equation is zero. (A more formal discussion of the conditions for a differential equation to have a solution satisfying boundary conditions is given in reference 16.) For the coefficient to be zero

$$w_1\left\{\frac{P^{(2)}}{b}\left(\frac{m\pi}{a}\right)^2 - \frac{Ehw_1^2}{16}\left[\left(\frac{m\pi}{a}\right)^4 + \left(\frac{n\pi}{b}\right)^4\right]\right\} = 0$$

The above relationship provides the means of determining the value of w_1. Ignoring the trivial case $w_1 = 0$, the amplitude w_1 is found to be

$$w_1^2 = \frac{16P^{(2)}}{Ehb} \frac{\left(\frac{m\pi}{a}\right)^2}{\left(\frac{m\pi}{a}\right)^4 + \left(\frac{n\pi}{b}\right)^4} \tag{19}$$

With what has been presented so far a first approximation to the solution of the large deflection behavior of the plate may be written if values are assigned to the perturbation parameter ϵ. This first approximation would include all powers of ϵ up to the second. The values chosen for ϵ and the results in equation form for the first approximation are indicated at the end of this section.

Upon satisfaction of relation (19), equation (18) may be solved directly for $w^{(3)}$ to give the following solution which satisfies boundary conditions

$$w^{(3)} = w_3 \sin \frac{m\pi x}{a} \sin \frac{n\pi y}{b} + w_{13}^{(3)} \sin \frac{m\pi x}{a} \sin \frac{3n\pi y}{b} + w_{31}^{(3)} \sin \frac{3m\pi x}{a} \sin \frac{n\pi y}{b} \tag{20}$$

where w_3 cannot be determined as yet, and

$$w_{13}^{(3)} = \frac{\frac{Ehw_1^2}{16}\left(\frac{m\pi}{a}\right)^4}{D\left[\left(\frac{m\pi}{a}\right)^2 + \left(\frac{3n\pi}{b}\right)^2\right]^2 - \frac{P^{(0)}}{b}\left(\frac{m\pi}{a}\right)^2}$$

$$w_{31}^{(3)} = \frac{\frac{Ehw_1^2}{16}\left(\frac{n\pi}{b}\right)^4}{D\left[\left(\frac{3m\pi}{a}\right)^2 + \left(\frac{n\pi}{b}\right)^2\right]^2 - \frac{P^{(0)}}{b}\left(\frac{3m\pi}{a}\right)^2}$$

The $N^{(13)}$ and the $N^{(31)}$ may now be found (in terms of w_3). Thus equation (8e) may be solved. From equations (8e) solutions that satisfy the boundary condition are

$$\begin{aligned} u^{(4)} = &-\left[\frac{P^{(4)}}{Ehb} + \frac{w_1 w_3}{4}\left(\frac{m\pi}{a}\right)^2\right]\left(x - \frac{a}{2}\right) - \frac{w_1 a}{8m\pi}\left\{w_3\left[\left(\frac{m\pi}{a}\right)^2 - \mu\left(\frac{n\pi}{b}\right)^2\right] + \right. \\ &\left. w_{31}^{(3)}\left[3\left(\frac{m\pi}{a}\right)^2 - \mu\left(\frac{n\pi}{b}\right)^2\right]\right\} \sin\frac{2m\pi x}{a} - \frac{w_1 w_{31}^{(3)} a}{16m\pi}\left[3\left(\frac{m\pi}{a}\right)^2 - \right. \\ &\left.\mu\left(\frac{n\pi}{b}\right)^2\right] \sin\frac{4m\pi x}{a} + \frac{w_1 m\pi}{8a}\left[w_3 - w_{13}^{(3)} + 3w_{31}^{(3)} - \right. \\ &\left. 4\left(\frac{n\pi}{b}\right)^2\left(w_{13}^{(3)} + w_{31}^{(3)}\right)\frac{\left(\frac{n\pi}{b}\right)^2 - \mu\left(\frac{m\pi}{a}\right)^2}{\left[\left(\frac{m\pi}{a}\right)^2 + \left(\frac{n\pi}{b}\right)^2\right]^2}\right]\sin\frac{2m\pi x}{a}\cos\frac{2n\pi y}{b} + \\ &\frac{w_1 w_{13}^{(3)} m\pi}{8a}\left[1 + \left(\frac{n\pi}{b}\right)^2\frac{4\left(\frac{n\pi}{b}\right)^2 - \mu\left(\frac{m\pi}{a}\right)^2}{\left[\left(\frac{m\pi}{a}\right)^2 + \left(\frac{2n\pi}{b}\right)^2\right]^2}\right]\sin\frac{2m\pi x}{a}\cos\frac{4n\pi y}{b} + \\ &\frac{w_1 w_{31}^{(3)} m\pi}{4a}\left[1 - \left(\frac{m\pi}{a}\right)^2\frac{4\left(\frac{m\pi}{a}\right)^2 + (2+\mu)\left(\frac{n\pi}{b}\right)^2}{\left[\left(\frac{2m\pi}{a}\right)^2 + \left(\frac{n\pi}{b}\right)^2\right]^2}\right]\sin\frac{4m\pi x}{a}\cos\frac{2n\pi y}{b} \end{aligned} \qquad (21)$$

$$v^{(4)} = \left[\frac{\mu P^{(4)}}{Ehb} - \frac{w_1 w_3}{4}\left(\frac{n\pi}{b}\right)^2\right]\left(y - \frac{b}{2}\right) - \frac{w_1 b}{8n\pi}\left\{w_3\left[\left(\frac{n\pi}{b}\right)^2 - \mu\left(\frac{m\pi}{a}\right)^2\right] + \right. \tag{21}$$

$$\left. w_{13}^{(3)}\left[3\left(\frac{n\pi}{b}\right)^2 - \mu\left(\frac{m\pi}{a}\right)^2\right]\right\} \sin\frac{2n\pi y}{b} - \frac{w_1 w_{13}^{(3)} b}{16n\pi}\left[3\left(\frac{n\pi}{b}\right)^2 - \right.$$

$$\left.\mu\left(\frac{m\pi}{a}\right)^2\right] \sin\frac{4n\pi y}{b} + \frac{w_1 n\pi}{8b}\left[w_3 - w_{31}^{(3)} + 3w_{13}^{(3)} - \right.$$

$$\left. 4\left(\frac{m\pi}{a}\right)^2\left(w_{31}^{(3)} + w_{13}^{(3)}\right)\frac{\left(\frac{m\pi}{a}\right)^2 - \mu\left(\frac{n\pi}{b}\right)^2}{\left[\left(\frac{m\pi}{a}\right)^2 + \left(\frac{n\pi}{b}\right)^2\right]^2}\right]\cos\frac{2m\pi x}{a}\sin\frac{2n\pi y}{b} +$$

$$\frac{w_1 w_{13}^{(3)} n\pi}{4b}\left[1 - \left(\frac{n\pi}{b}\right)^2\frac{4\left(\frac{n\pi}{b}\right)^2 + (2+\mu)\left(\frac{m\pi}{a}\right)^2}{\left[\left(\frac{m\pi}{a}\right)^2 + \left(\frac{2n\pi}{b}\right)^2\right]^2}\right]\cos\frac{2m\pi x}{a}\sin\frac{4n\pi y}{b} +$$

$$\frac{w_1 w_{31}^{(3)} n\pi}{8b}\left[1 + \left(\frac{m\pi}{a}\right)^2\frac{4\left(\frac{m\pi}{a}\right)^2 - \mu\left(\frac{n\pi}{b}\right)^2}{\left[\left(\frac{2m\pi}{a}\right)^2 + \left(\frac{n\pi}{b}\right)^2\right]^2}\right]\cos\frac{4m\pi x}{a}\sin\frac{2n\pi y}{b}$$

so that

$$N_x^{(4)} + 2N_x^{(13)} = -\frac{P^{(4)}}{b} - \frac{Ehw_1}{4}\left(\frac{m\pi}{a}\right)^2\left[\left(w_3 - w_{13}^{(3)}\right)\cos\frac{2n\pi y}{b} + w_{13}^{(3)}\cos\frac{4n\pi y}{b} + \frac{4\left(w_{13}^{(3)} + w_{31}^{(3)}\right)\left(\frac{n\pi}{b}\right)^4}{\left[\left(\frac{m\pi}{a}\right)^2 + \left(\frac{n\pi}{b}\right)^2\right]^2}\cos\frac{2m\pi x}{a}\cos\frac{2n\pi y}{b} - \frac{4w_{13}^{(3)}\left(\frac{n\pi}{b}\right)^4}{\left[\left(\frac{m\pi}{a}\right)^2 + \left(\frac{2n\pi}{b}\right)^2\right]^2}\cos\frac{2m\pi x}{a}\cos\frac{4n\pi y}{b} - \frac{w_{31}^{(3)}\left(\frac{n\pi}{b}\right)^4}{\left[\left(\frac{2m\pi}{a}\right)^2 + \left(\frac{n\pi}{b}\right)^2\right]^2}\cos\frac{4m\pi x}{a}\cos\frac{2n\pi y}{b}\right]$$

$$N_y^{(4)} + 2N_y^{(13)} = -\frac{Ehw_1}{4}\left(\frac{n\pi}{b}\right)^2\left[\left(w_3 - w_{31}^{(3)}\right)\cos\frac{2m\pi x}{a} + w_{31}^{(3)}\cos\frac{4m\pi x}{a} + \frac{4\left(w_{13}^{(3)} + w_{31}^{(3)}\right)\left(\frac{m\pi}{a}\right)^4}{\left[\left(\frac{m\pi}{a}\right)^2 + \left(\frac{n\pi}{b}\right)^2\right]^2}\cos\frac{2m\pi x}{a}\cos\frac{2n\pi y}{b} - \frac{w_{13}^{(3)}\left(\frac{m\pi}{a}\right)^4}{\left[\left(\frac{m\pi}{a}\right)^2 + \left(\frac{2n\pi}{b}\right)^2\right]^2}\cos\frac{2m\pi x}{a}\cos\frac{4n\pi y}{b} - \frac{4w_{31}^{(3)}\left(\frac{m\pi}{a}\right)^4}{\left[\left(\frac{2m\pi}{a}\right)^2 + \left(\frac{n\pi}{b}\right)^2\right]^2}\cos\frac{4m\pi x}{a}\cos\frac{2n\pi y}{b}\right] \quad (22)$$

$$N_{xy}^{(4)} + N_{xy}^{(13)} + N_{xy}^{(31)} = -\frac{Ehw_1}{2}\left(\frac{m\pi}{a}\frac{n\pi}{b}\right)^2 \left[\frac{2\left(w_{13}^{(3)} + w_{31}^{(3)}\right)}{\left[\left(\frac{m\pi}{a}\right)^2 + \left(\frac{n\pi}{b}\right)^2\right]^2} \sin\frac{2m\pi x}{a} \sin\frac{2n\pi y}{b} - \right.$$

$$\frac{w_{13}^{(3)}}{\left[\left(\frac{m\pi}{a}\right)^2 + \left(\frac{2n\pi}{b}\right)^2\right]^2} \sin\frac{2m\pi x}{a} \sin\frac{4n\pi y}{b} -$$

$$\left. \frac{w_{31}^{(3)}}{\left[\left(\frac{2m\pi}{a}\right)^2 + \left(\frac{n\pi}{b}\right)^2\right]^2} \sin\frac{4m\pi x}{a} \sin\frac{2n\pi y}{b} \right]$$

The differential equation (8f) is now completely determined except for $w^{(5)}$ and w_3. The condition that this equation has a solution for $w^{(5)}$ determines the value of w_3 in the same way that the condition that equation (18) has a solution determined the value of w_1.

$$w_3 = \frac{\left(\frac{m\pi}{a}\right)^4 w_{13}^{(3)} + \left(\frac{n\pi}{b}\right)^4 w_{31}^{(3)} + \frac{16P^{(4)}}{3Ehbw_1}\left(\frac{m\pi}{a}\right)^2}{\left(\frac{m\pi}{a}\right)^4 + \left(\frac{n\pi}{b}\right)^4 - \frac{16P^{(2)}}{3Ehbw_1^2}\left(\frac{m\pi}{a}\right)^2} \qquad (23)$$

The second approximation may now be written if values are assigned to the perturbation parameter ϵ. The second approximation would include all powers of ϵ up to the fourth. The formal solution of the set (8) is not carried beyond this point for the compression problem.

Nothing has been said so far in this section about what values the parameter ϵ assumes except that it is arbitrary. Since P is the

known total applied load, the magnitude of which has not been specified except to say that it is equal to or above the buckling load, ϵ may be related to P as in the following equation without loss of generality

$$\epsilon^2 = \frac{P - P_{cr}}{P_{cr}} \tag{24}$$

where P_{cr} is the buckling load which can be identified as equal to $P^{(0)}$ for given values of m and n. With $P^{(0)} = P_{cr}$ equation (24) can be written

$$P = P^{(0)} + \epsilon^2 P^{(0)}$$

Equating coefficients of equal powers of ϵ in the above equation with that of equation (9) yields

$$P^{(2)} = P^{(0)}$$

$$P^{(n)} = 0 \quad \text{for} \quad n \geq 4$$

Alternatively, if ϵ had been related instead either to the center deflection or to the shortening of the loaded edges or to some other characteristic property of the plate loading, then that relation would determine the $P^{(n)}$. In any case, the final results would be unchanged.

In the following, results for the deflections and stresses are written in equation form for the second approximation.

$$u = -\frac{\pi^2}{3(1-\mu^2)}\frac{h^2 a}{b^2}\left(\frac{Pb}{4D\pi^2}\left(\frac{x}{a}-\frac{1}{2}\right)+\delta^2\left[\frac{\beta^2}{2}\left(\frac{x}{a}-\frac{1}{2}\right)+\frac{\beta^2-\mu n^2}{4m\pi}\sin\frac{2m\pi x}{a}-\right.\right.$$

$$\frac{\beta^2}{4m\pi}\sin\frac{2m\pi x}{a}\cos\frac{2n\pi y}{b}\Bigg]+\delta^4\left\{\bar{w}_3\beta^2\left(\frac{x}{a}-\frac{1}{2}\right)+\frac{1}{2m\pi}\left[\bar{w}_3\left(\beta^2-\mu n^2\right)+\right.\right.$$

$$\left.\left.\bar{w}_{31}^{(3)}(3\beta^2-\mu n^2)\right]\sin\frac{2m\pi x}{a}+\frac{1}{4m\pi}\bar{w}_{31}^{(3)}(3\beta^2-\mu n^2)\sin\frac{4m\pi x}{a}-\right.$$

$$\frac{\beta^2}{2m\pi}\left[\bar{w}_3-\bar{w}_{13}^{(3)}+3\bar{w}_{31}^{(3)}-\left(\bar{w}_{13}^{(3)}+\bar{w}_{31}^{(3)}\right)\frac{4n^2(n^2-\mu\beta^2)}{(\beta^2+n^2)^2}\right]\sin\frac{2m\pi x}{a}$$

$$\cos\frac{2n\pi y}{b}-\frac{\beta^2}{2m\pi}\bar{w}_{13}^{(3)}\left(1+\frac{n^2(4n^2-\mu\beta^2)}{(\beta^2+4n^2)^2}\right)\sin\frac{2m\pi x}{a}\cos\frac{4n\pi y}{b}-$$

$$\left.\left.\frac{\beta^2}{m\pi}\bar{w}_{31}^{(3)}\left(1-\frac{\beta^2\left[4\beta^2+(2+\mu)n^2\right]}{(4\beta^2+n^2)^2}\right)\sin\frac{4m\pi x}{a}\cos\frac{2n\pi y}{b}\right\}\right) \qquad (25)$$

(25)

$$v = -\frac{\pi^2}{3(1-\mu^2)}\frac{h^2}{b}\left(-\frac{\mu P b}{4D\pi^2}\left(\frac{y}{b}-\frac{1}{2}\right)+\delta^2\left[\frac{n^2}{2}\left(\frac{y}{b}-\frac{1}{2}\right)+\frac{n^2-\mu\beta^2}{4n\pi}\sin\frac{2n\pi y}{b}-\right.\right.$$

$$\left.\frac{n}{4\pi}\cos\frac{2m\pi x}{a}\sin\frac{2n\pi y}{b}\right]+\delta^4\left\{\bar{w}_3 n^2\left(\frac{y}{b}-\frac{1}{2}\right)+\frac{1}{2n\pi}\left[\bar{w}_3(n^2-\mu\beta^2)+\right.\right.$$

$$\left.\bar{w}_{13}^{(3)}(3n^2-\mu\beta^2)\right]\sin\frac{2n\pi y}{b}+\frac{1}{4n\pi}\bar{w}_{13}^{(3)}(3n^2-\mu\beta^2)\sin\frac{4n\pi y}{b}-$$

$$\frac{n}{2\pi}\left[\bar{w}_3-\bar{w}_{31}^{(3)}+3\bar{w}_{13}^{(3)}-\left(\bar{w}_{13}^{(3)}+\bar{w}_{31}^{(3)}\right)\frac{4\beta^2(\beta^2-\mu n^2)}{(\beta^2+n^2)^2}\right]\cos\frac{2m\pi x}{a}$$

$$\sin\frac{2n\pi y}{b}-\frac{n}{\pi}w_{13}^{(3)}\left(1-\frac{n^2\left[4n^2+(2+\mu)\beta^2\right]}{(\beta^2+4n^2)^2}\right)\cos\frac{2m\pi x}{a}\sin\frac{4n\pi y}{b}-$$

$$\left.\left.\frac{n}{2\pi}\bar{w}_{31}^{(3)}\left(1+\frac{\beta^2(4\beta^2-\mu n^2)}{(4\beta^2+n^2)^2}\right)\cos\frac{4m\pi x}{a}\sin\frac{2n\pi y}{b}\right\}\right)$$

$$w = \frac{2h\delta}{\sqrt{3(1-\mu^2)}}\left[\sin\frac{m\pi x}{a}\sin\frac{n\pi y}{b}+\delta^2\left(\bar{w}_3\sin\frac{m\pi x}{a}\sin\frac{n\pi y}{b}+\bar{w}_{13}^{(3)}\right.\right.$$

$$\left.\left.\sin\frac{m\pi x}{a}\sin\frac{3n\pi y}{b}+\bar{w}_{31}^{(3)}\sin\frac{3m\pi x}{a}\sin\frac{n\pi y}{b}\right)\right]$$

$$
\begin{aligned}
N_x = &- \frac{P}{b} - \frac{D\pi^2}{b^2}\left\{2\beta^2\delta^2 \cos\frac{2n\pi y}{b} + 4\beta^2\delta^4\left[\left(\bar{w}_3 - \bar{w}^{(3)}_{13}\right)\cos\frac{2n\pi y}{b} + \bar{w}^{(3)}_{13}\right.\right. \\
&\cos\frac{4n\pi y}{b} + \frac{4n^4\left(\bar{w}^{(3)}_{13} + \bar{w}^{(3)}_{31}\right)}{\left(\beta^2 + n^2\right)^2}\cos\frac{2m\pi x}{a}\cos\frac{2n\pi y}{b} - \frac{4n^4\bar{w}^{(3)}_{13}}{\left(\beta^2 + 4n^2\right)^2} \\
&\left.\left.\cos\frac{2m\pi x}{a}\cos\frac{4n\pi y}{b} - \frac{n^4\bar{w}^{(3)}_{31}}{\left(4\beta^2 + n^2\right)^2}\cos\frac{4m\pi x}{a}\cos\frac{2n\pi y}{b}\right]\right\} \\
N_y = &- \frac{D\pi^2}{b^2}\left\{2n^2\delta^2 \cos\frac{2m\pi x}{a} + 4n^2\delta^4\left[\left(\bar{w}_3 - \bar{w}^{(3)}_{31}\right)\cos\frac{2m\pi x}{a} + \bar{w}^{(3)}_{31}\right.\right. \\
&\cos\frac{4m\pi x}{a} + \frac{4\beta^4\left(\bar{w}^{(3)}_{13} + \bar{w}^{(3)}_{31}\right)}{\left(\beta^2 + n^2\right)^2}\cos\frac{2m\pi x}{a}\cos\frac{2n\pi y}{b} - \frac{\beta^4\bar{w}^{(3)}_{13}}{\left(\beta^2 + 4n^2\right)^2} \\
&\left.\left.\cos\frac{2m\pi x}{a}\cos\frac{4n\pi y}{b} - \frac{4\beta^4\bar{w}^{(3)}_{31}}{\left(4\beta^2 + n^2\right)^2}\cos\frac{4m\pi x}{a}\cos\frac{2n\pi y}{b}\right]\right\} \\
N_{xy} = &-8\delta^4\beta^3n^3\frac{D\pi^2}{b^2}\left(\frac{2\left(\bar{w}^{(3)}_{13} + \bar{w}^{(3)}_{31}\right)}{\left(\beta^2 + n^2\right)^2}\sin\frac{2m\pi x}{a}\sin\frac{2n\pi y}{b} - \frac{\bar{w}^{(3)}_{13}}{\left(\beta^2 + 4n^2\right)^2}\right. \\
&\left.\sin\frac{2m\pi x}{a}\sin\frac{4n\pi y}{b} - \frac{\bar{w}^{(3)}_{31}}{\left(4\beta^2 + n^2\right)^2}\sin\frac{4m\pi x}{a}\sin\frac{2n\pi y}{b}\right)
\end{aligned}
\tag{26}
$$

where

$$\delta^2 = \frac{\beta^2 \frac{Pb}{D\pi^2} - (\beta^2 + n^2)^2}{\beta^4 + n^4}$$

$$\beta = \frac{mb}{a}$$

$$\bar{w}_3 = \frac{3}{2} \frac{\beta^4 \bar{w}_{13}^{(3)} + n^4 \bar{w}_{31}^{(3)}}{\beta^4 + n^4}$$

$$\bar{w}_{13}^{(3)} = \frac{\beta^4}{(\beta^2 + 9n^2)^2 - (\beta^2 + n^2)^2}$$

$$\bar{w}_{31}^{(3)} = \frac{n^4}{(9\beta^2 + n^2)^2 - 9(\beta^2 + n^2)^2}$$

In order to get the first approximation results from the equations given above for the second approximation, simply omit the part of w that has the coefficient δ^3 and the parts of the other results that have the coefficient δ^4.

Several results of interest will now be written down in second approximation. To obtain the first approximation from these results omit the highest power of δ appearing. The total shortening Δ is the sum of the inward displacements at each end. Since u is positive in the x direction

$$\Delta = u(o,y) - u(a,y) \qquad (27)$$

Therefore

$$\frac{3(1-\mu^2)}{\pi^2}\frac{b^2}{h^2}\frac{\Delta}{a} = \frac{Pb}{4\pi^2 D} + \frac{\delta^2\beta^2}{2} + \delta^4\bar{w}_3\beta^2 \tag{28}$$

The extreme fiber bending strain at the crest of a buckle ϵ_{x_b} is given by

$$\epsilon_{x_b} = \pm\frac{h}{2}\, w_{,xx}\left(\frac{a}{2m}, \frac{b}{2n}\right)$$

or

$$\frac{3(1-\mu^2)}{\pi^2}\frac{b^2}{h^2}\epsilon_{x_b} = \pm\beta^2\delta\sqrt{3(1-\mu^2)}\left[1 + \delta^2\left(\bar{w}_3 - \bar{w}_{13}^{(3)} + 9\bar{w}_{31}^{(3)}\right)\right] \tag{29}$$

The extreme fiber compressive strain at the crest of a buckle ϵ_{x_o} is the sum of the middle surface strain and the bending strain just given. The middle surface strain may be obtained in two ways from the results for deflections and stresses just given. It may be obtained by differentiation of the deformations (equations (4)) or by calculating it in terms of stresses (equations (2)). The results obtained will be different for a given approximation depending on which way it is done. For example, for the second approximation, the sixth power of ϵ would appear in the middle surface strains if they are calculated from equations (4) while only the fourth power of ϵ would appear if equations (2) are used. Of course, in the limit the results will agree. The most consistent way for a given approximation would be by equation (2); consistent powers of ϵ appear. This yields,

$$\epsilon_{x_o} = -\frac{1}{Eh}\left[N_x\left(\frac{a}{2m}, \frac{b}{2n}\right) - \mu N_y\left(\frac{a}{2m}, \frac{b}{2n}\right)\right] + \epsilon_{x_b}$$

Therefore

$$\frac{3(1-\mu^2)}{\pi^2}\frac{b^2}{h^2}\epsilon_{x_o} = \frac{Pb}{4\pi^2 D} - \frac{1}{2}(\beta^2 - \mu n^2)\delta^2 + \delta^4\left[2\beta^2\bar{w}_{13}^{(3)} - 2\mu n^2\bar{w}_{31}^{(3)} - (\beta^2 - \mu n^2)\bar{w}_3 + \frac{4\left(n^4 - \mu\beta^4\right)\left(\bar{w}_{13}^{(3)} + \bar{w}_{31}^{(3)}\right)}{\left(\beta^2 + n^2\right)^2} + \frac{\left(4n^4 - \mu\beta^4\right)\bar{w}_{13}^{(3)}}{\left(\beta^2 + 4n^2\right)^2} + \frac{\left(n^4 - 4\mu\beta^4\right)\bar{w}_{31}^{(3)}}{\left(4\beta^2 + n^2\right)^2}\right] + \frac{3(1-\mu^2)}{\pi^2}\frac{b^2}{h^2}\epsilon_{x_b} \tag{30}$$

The effective width b_e as defined below (see ref. 14, for example) may also be of interest.

$$b_e = \frac{P}{F\Delta}\frac{a}{h}$$

Substituting from (28) for Δ results in

$$\frac{b_e}{b} = \frac{\frac{Pb}{4\pi^2 D}}{\frac{Pb}{4\pi^2 D} + \delta^2\frac{\beta^2}{2} + \delta^4\bar{w}_3\beta^2} \tag{31}$$

B. Results

To use the equations just derived, m, the number of buckles along the length, and n, the number of buckles along the width, must be

determined. At buckling the small deflection (linear) theory determines the values of m and n to use as the ones which yield the lowest buckling load. Load-shortening curves are shown for both the first and second approximation in Figure 1 for plates of various finite length-width ratios using the values of m (n always equals unity for this problem) for lowest buckling load. In addition, load-shortening curves are given for other values of m which intersect with these basic curves for the range plotted.

These intersections indicate possible changes in buckle pattern. For finite plates, changes in buckle pattern are often noted experimentally, and they will be discussed theoretically in a following section. For an infinitely long plate the number of buckles along the length is infinite ($m \rightarrow \infty$), but the ratio of the number of buckles to the length, $\frac{m}{a}$, is finite. The inverse of this ratio is the buckle length $\frac{a}{m}$ and for infinite plates it would be expected that there is continuous change in buckle length as the loading progresses[7,9]. The buckle length for a given shortening would be such that the load is a minimum. Values of the ratio $\beta = \frac{mb}{a}$ for minimum load and the corresponding values of load and shortening are given in the following table. These values were used to plot the load-shortening curves for the infinite plate in Figure 1. Note that the results giving the lowest load for a given shortening for length-width ratio 2 and 4 do not differ much from the infinite plate results. Indeed, the infinite plate curves form an envelope for the finite plate curves.

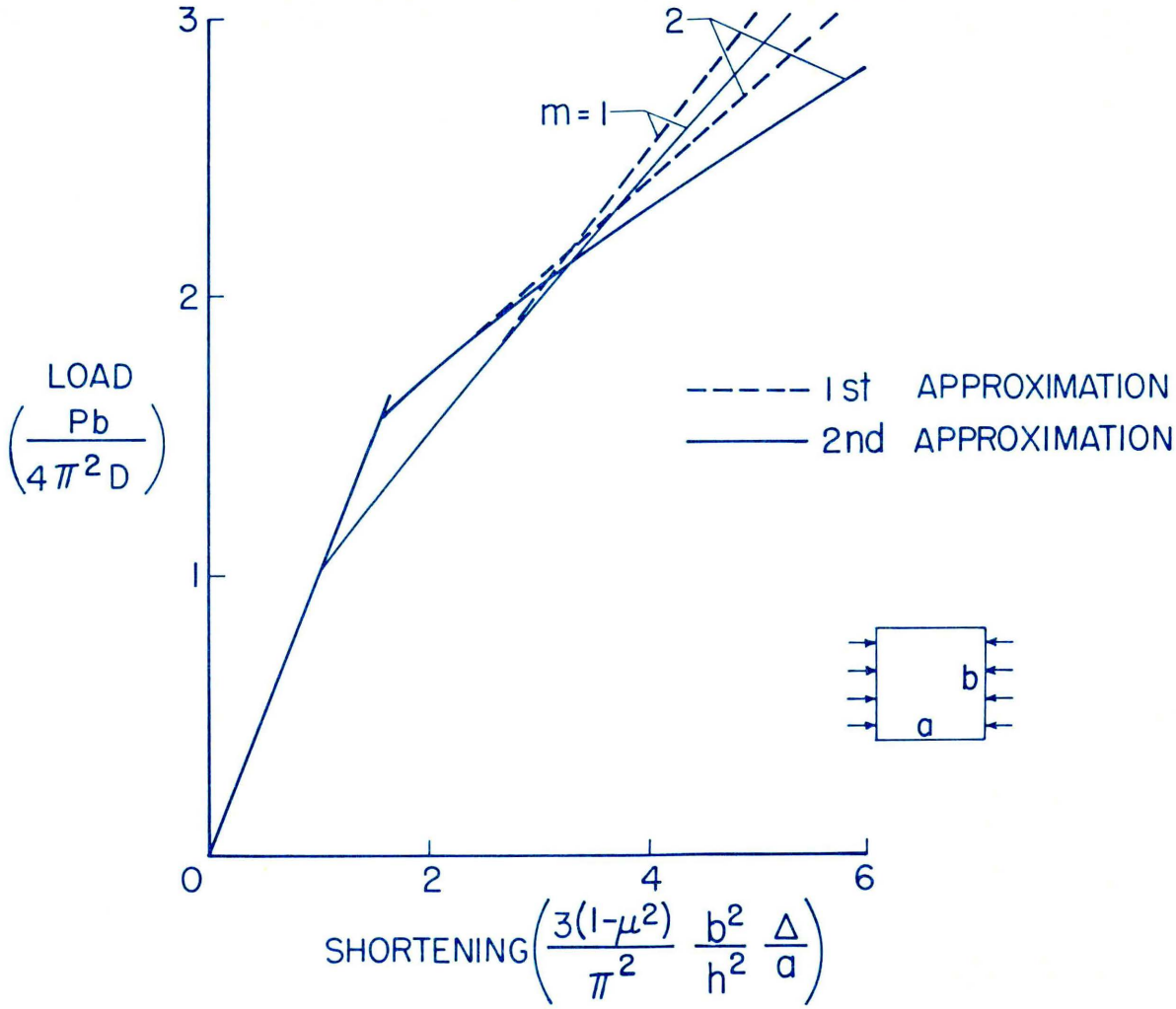

(a) a/b = 1.

Figure 1.- Load-shortening curves of rectangular simply supported plates in compression.

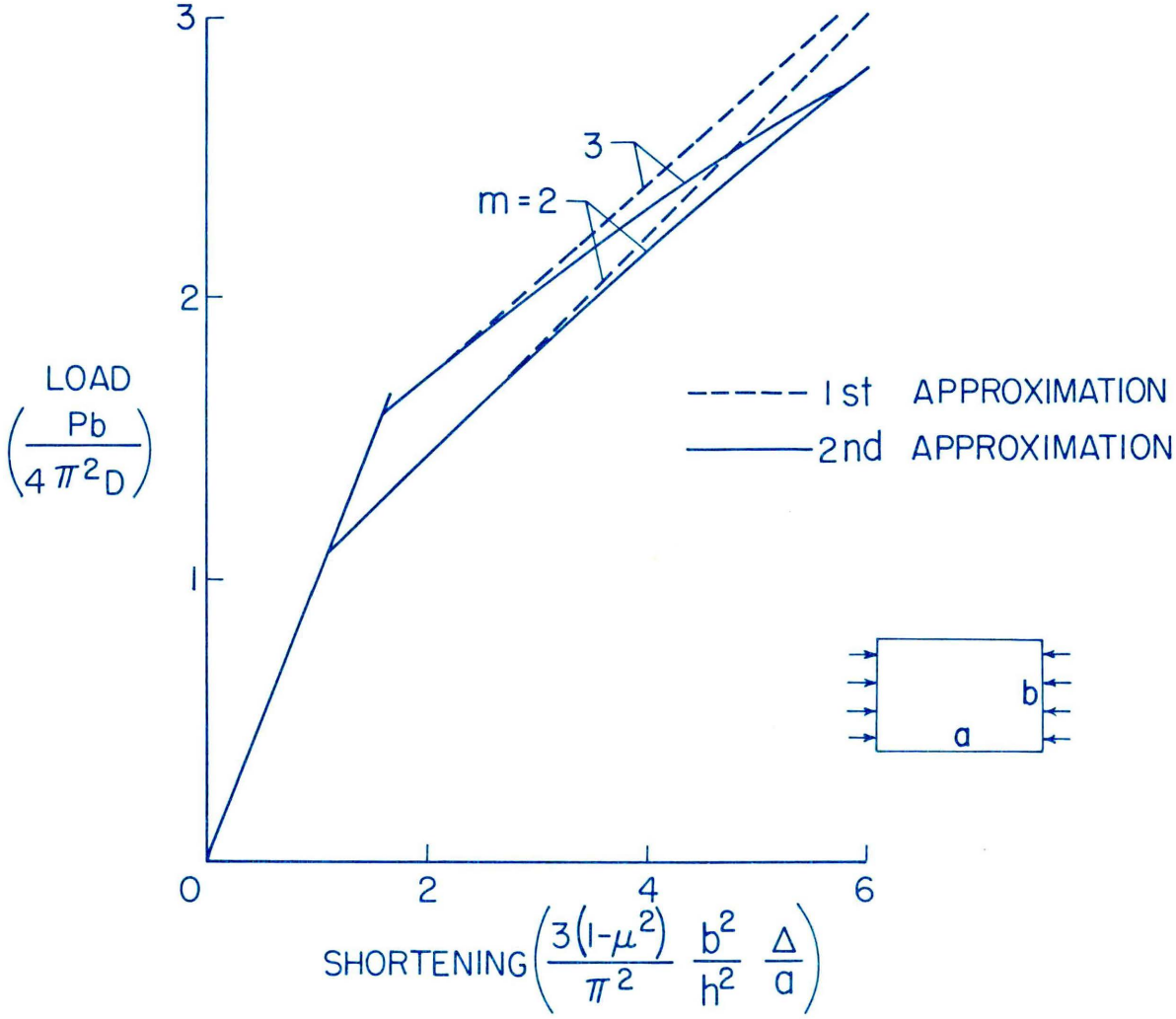

(b) a/b = 1.5.

Figure 1.- Continued.

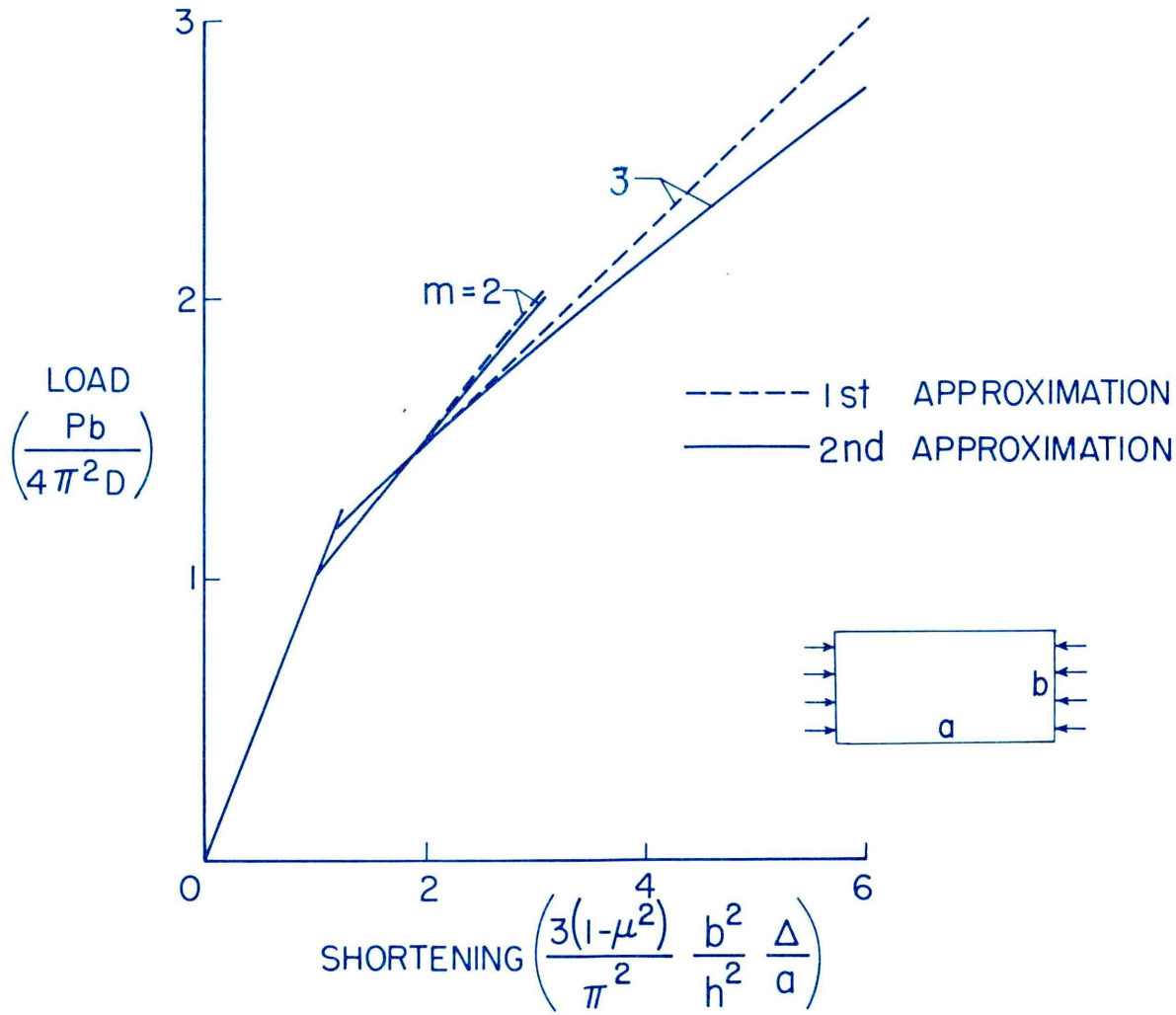

(c) a/b = 2.

Figure 1.- Continued.

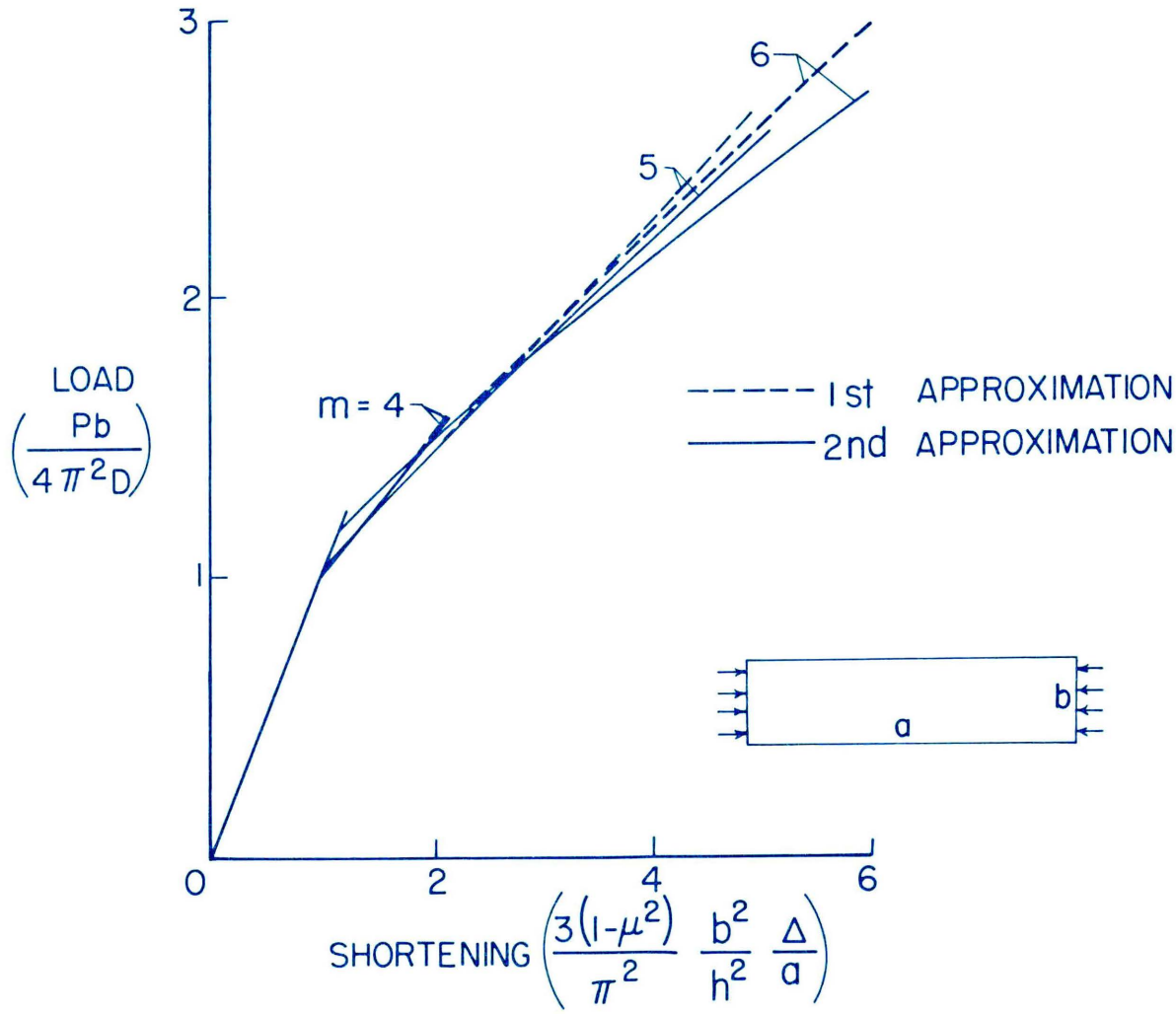

(d) a/b = 4.

Figure 1.- Continued.

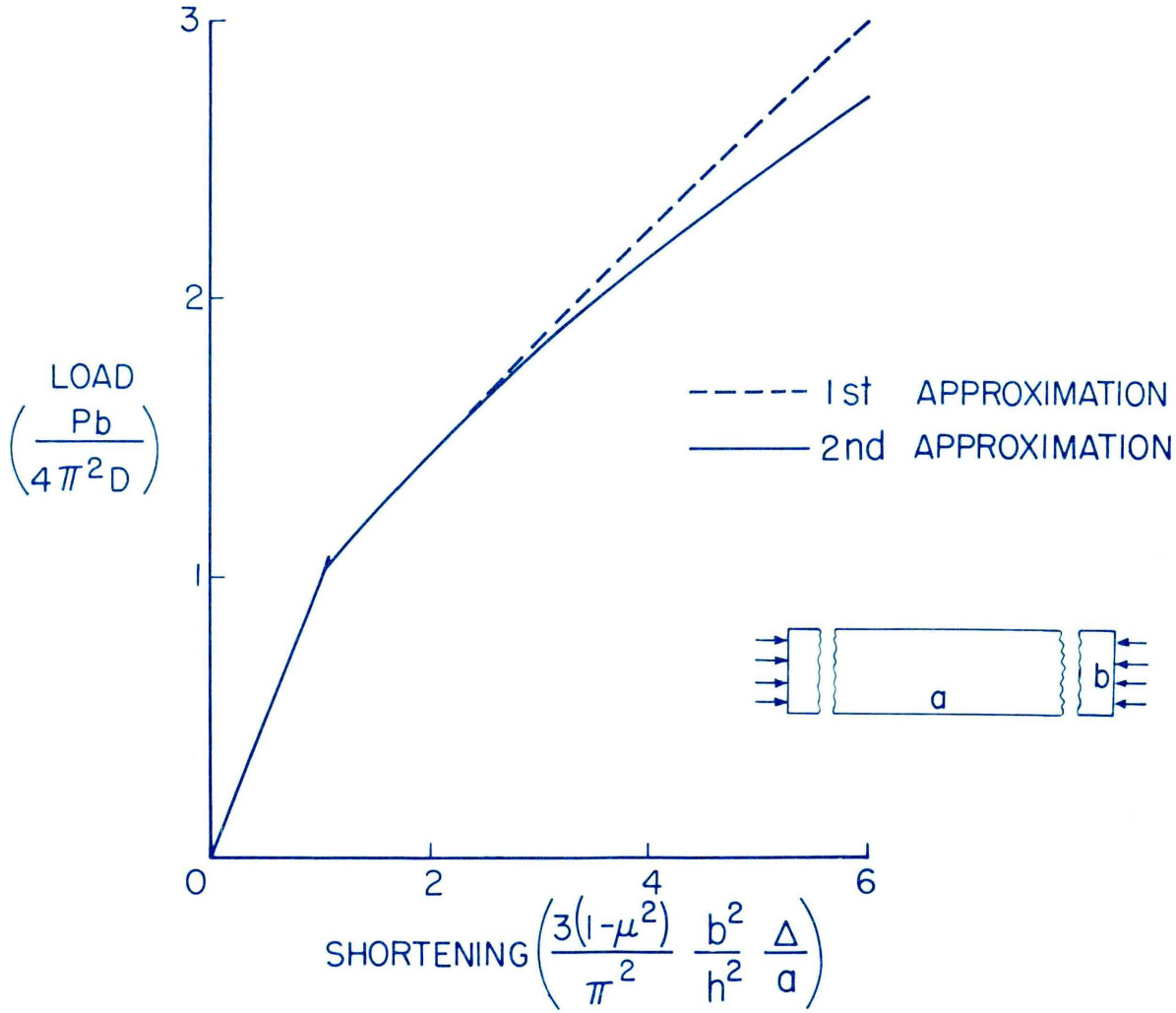

(e) $a/b \to \infty$.

Figure 1.- Concluded.

TABLE I

BUCKLE LENGTH RATIO β AND CORRESPONDING LOADS AND SHORTENINGS FOR AN INFINITELY LONG SIMPLY SUPPORTED PLATE IN LONGITUDINAL COMPRESSION

$\frac{Pb}{4\pi^2 D}$	1st Approximation		2nd Approximation	
	β	$\frac{3(1-\mu^2)}{\pi^2}\frac{b^2}{h^2}\frac{\Delta}{a}$	β	$\frac{3(1-\mu^2)}{\pi^2}\frac{b^2}{h^2}\frac{\Delta}{a}$
1	1	1	1	1
1.05	1.045	1.10	1.045	1.10
1.33	1.20	1.73	1.20	1.74
1.61	1.30	2.41	1.31	2.46
1.95	1.39	3.27	1.42	3.42
2.25	1.45	4.05	1.51	4.37
2.68	1.52	5.20	1.64	5.88

An indication of the convergence of the results of such an analysis is the agreement between the last approximation and the previous approximation. From Figure 1, good convergence is indicated in the range plotted since the curves of the first and second approximation lie reasonably close together. Convergence is better for nearly square buckles than for higher values of $\frac{mb}{a}$.

Comparisons with other theory and with experiment will be discussed later in this dissertation.

C. Extensions to Other Problems

In the foregoing example problem all of the differential equations were solved by inspection (the solution could be identified from the usual form of the equations and the boundary conditions). The steps in the analysis of a given problem are essentially the same independent of the method of solution of each of the differential equations involved. Of course, for some other problems, it might be necessary to solve the differential equations by other methods.

For the example problem the aribtrary parameter ϵ was taken equal to the square root of $(P - P_{cr})/P_{cr}$. It could just as well have been related to the shortening or the center deflection. For other problems it may be convenient to relate the arbitrary parameter to some other property. For example in a thermal buckling problem (as shown later) the arbitrary parameter may be related to the average rise in temperature beyond that required for buckling.

There are problems for which similar expansions in series do not lead to linear equations, such as for the study of the postbuckling

behavior of a rectangular plate with initial eccentricities or with lateral load. For such cases other methods must be used. There are problems for which similar expansions do lead to linear equations, but there may be ranges where results from these equations do not converge rapidly. The usefulness of the set of linear equations obtained or the method used in this dissertation to obtain the set will depend then to a great extent on the type of large deflection problem it is desired to solve.

VIII. THE PHENOMENON OF CHANGE IN BUCKLE PATTERN

Several authors (see refs. 13, 14, and 15) have considered the phenomenon of change of buckle pattern. All agree that changes may occur when there are intersections of load-shortening curves for the various modes of buckling. Obviously, the plate will stay in the original mode until it becomes unstable. Alexeev[13] surmises that the actual transitions from one mode to another would be displaced from the load or shortening given by the intersection of load-shortening curves (for the various modes of buckling) depending on the condition of the experiment and initial imperfections. On the other hand, van der Neut[15] conjectures that the actual transition would occur near the point when the area under the load-shortening curves for each of the modes becomes equal depending on the initial imperfections. Cox[16] presents a two mode solution in which he obtained a transition curve between the load-shortening curve of the two modes and he suggests that the change would start from the intersection of the curve for the first mode and the transition curve. There have been no rigorous studies made of change in buckle pattern, and the mechanism of change has not been described.

In order to resolve questions concerned with change in buckle pattern a simple model was chosen which exhibits the important properties associated with this phenomenon. This model was chosen so that an exact solution could be obtained. The analysis of the model, including a rigorous study of stability in its various modes, follows.

A. Analysis of Simple Model

The model considered is a column consisting of three rigid rods connected by linear torsional springs and supported along the length by nonlinear extensional springs as shown in Figure 2. The rods considered are of equal length, and the restoring force of each of the nonlinear springs is taken to be proportional to the cube of its displacement. The stability of this column will be investigated for both the controlled load and controlled shortening types of load application.

Since the stability is of interest, it is convenient to use an energy approach. The equilibrium configurations, that is, those configurations for which the potential energy is an extremum, will be found. These extremums will then be investigated to see which of them are minimums (and hence imply stability) and which are otherwise (and hence imply instability). Solutions will be presented in the form of load-shortening curves giving results for the various spring stiffnesses.

The potential energy is set up for each of the elements of the system then summed up to obtain the total potential energy. For the nonlinear springs the force in the spring is proportional to the cube of the displacement of the spring, that is, in the form

$$F = Kw^3$$

The strain energy in a spring is related to the force and displacement as given in the following expression

$$\int_0^w F \, dw$$

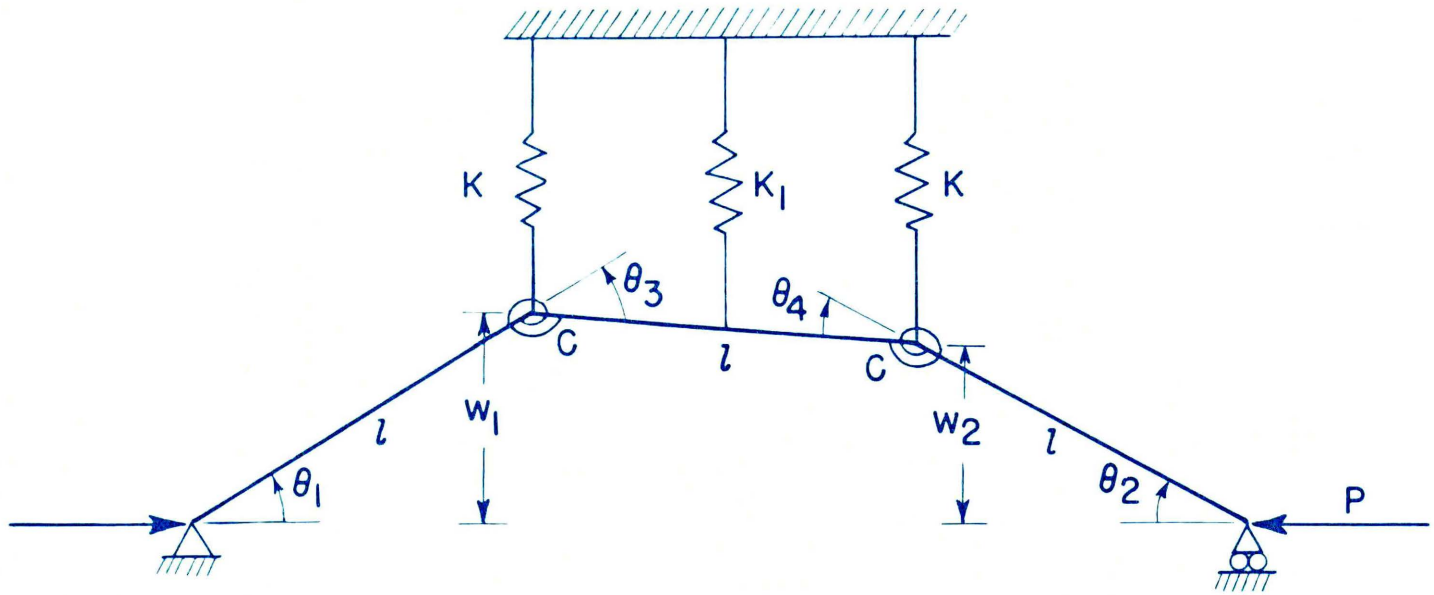

Figure 2.- Three element column connected by linear torsional springs and laterally restrained by nonlinear extensional springs.

Thus, the potential (strain) energy of the nonlinear springs is

$$\Pi_1 = \frac{K}{4}\left(w_1^4 + w_2^4\right) + \frac{K_1}{4}\left(\frac{w_1 + w_2}{2}\right)^4 \tag{32}$$

With the assumption that the deflections are small compared to the length of the column, the angles are given in terms of the deflections by

$$\theta_1 = \frac{w_1}{l}$$

$$\theta_2 = \frac{w_2}{l}$$

$$\theta_3 = \frac{2w_1 - w_2}{l}$$

$$\theta_4 = \frac{2w_2 - w_1}{l}$$

Making use of this assumption, the potential (strain) energy of the torsional springs can be written

$$\Pi_2 = \frac{C}{2}\left[\left(\frac{2w_1 - w_2}{l}\right)^2 + \left(\frac{2w_2 - w_1}{l}\right)^2\right] \tag{33}$$

The shortening Δ of the column is

$$\Delta = l\left\{3 - \left[\cos\theta_1 + \cos\theta_2 + \cos\left(\theta_1 + \theta_2\right)\right]\right\}$$

or with the assumption of small deflections

$$\Delta = \frac{1}{2l}\left[w_1^2 + w_2^2 + \left(w_1 - w_2\right)^2\right] \tag{34}$$

The potential energy of the load P is the negative product of load and shortening

$$\Pi_3 = -\frac{P}{2l}\left[w_1^2 + w_2^2 + \left(w_1 - w_2\right)^2\right] \tag{35}$$

Before proceeding to use the energies just written, it is convenient to replace w_1 and w_2 by ξ and η according to

$$\xi = \frac{w_1 + w_2}{2}$$

$$\eta = \frac{w_1 - w_2}{2}$$

Note that when $\eta = 0$ the deflections are symmetric, and when $\xi = 0$ the deflections are antisymmetric. In terms of the new variables the energies (32), (33), and (35) become

$$\Pi_1 = \frac{K}{2}\left(\xi^4 + 6\xi^2\eta^2 + \eta^4\right) + \frac{K_1}{4}\xi \tag{36}$$

$$\Pi_2 = \frac{C}{l^2}\left(\xi^2 + 9\eta^2\right) \tag{37}$$

$$\Pi_3 = -\frac{P}{l}\left(\xi^2 + 3\eta^2\right) \tag{38}$$

and the shortening (34) becomes

$$\Delta = \frac{1}{l}\left(\xi^2 + 3\eta^2\right) \tag{39}$$

The total potential energy is

$$\Pi = \Pi_1 + \Pi_2 + \Pi_3$$

for the controlled load case and

$$\Pi = \Pi_1 + \Pi_2$$

for the controlled shortening case. For the latter case the potential energy is equal to the strain energy of the system.

1. Controlled load.- According to the minimum potential energy method the variation of the total potential energy of the system must vanish.

$$\delta\Pi = \frac{\partial\Pi}{\partial\xi}\,\delta\xi + \frac{\partial\Pi}{\partial\eta}\,\delta\eta = 0$$

Since the variation of ξ and η are perfectly arbitrary

$$\frac{\partial\Pi}{\partial\xi} = 0$$

$$\frac{\partial\Pi}{\partial\eta} = 0$$

Thus, the following conditions for buckling are obtained

$$\left.\begin{aligned} 0 &= \xi\left[K\left(\xi^2 + 3\eta^2\right) + \frac{K_1}{2}\,\xi^2 + \frac{C}{l^2} - \frac{P}{l}\right] \\ 0 &= \eta\left[K\left(3\xi^2 + \eta^2\right) + 9\,\frac{C}{l^2} - 3\,\frac{P}{l}\right] \end{aligned}\right\} \qquad (40)$$

A possible solution is

$$\eta = 0$$

with

$$\xi^2 = \frac{2C}{l^2K}\left(\frac{\frac{Pl}{C} - 1}{2 + \frac{K_1}{K}}\right) \tag{41}$$

Another possible solution is

$$\xi = 0$$

with

$$\eta^2 = \frac{3C}{l^2K}\left(\frac{Pl}{C} - 3\right) \tag{42}$$

And there exists a possible third solution where ξ and η are both not equal to zero but are given by

$$\xi^2 = \frac{4C}{l^2K}\left(\frac{4\,\frac{Pl}{C} - 13}{16 - \frac{K_1}{K}}\right)$$

$$\eta^2 = \frac{3CK_1}{l^2K^2}\left(\frac{4\,\frac{K}{K_1} + 3 - \frac{Pl}{C}}{16 - \frac{K_1}{K}}\right) \tag{43}$$

This solution gives deflections which are neither symmetric nor anti-symmetric. Note that for the various possible solutions, limitations may be set down immediately on the ranges of loading which may be considered. Real values of ξ and η and therefore of the deflections w_1 and w_2 will occur in the first solution only if $\frac{Pl}{C} > 1$, in the

second if $\frac{Pl}{C} > 3$ and in the third if either $\left(4\frac{K}{K_1} + 3\right) > \frac{Pl}{C} > \frac{13}{4}$ for $K_1 < 16K$ or $\left(4\frac{K}{K_1} + 3\right) < \frac{Pl}{C} < \frac{13}{4}$ for $K_1 > 16K$. In these ranges the three solutions represent equilibrium positions.

The shortening (39) can now be written for each of the three solutions.

For $\eta = 0$

$$\frac{Kl^3\Delta}{C} = 2\left(\frac{\frac{Pl}{C} - 1}{2 + \frac{K_1}{K}}\right) \tag{44}$$

For $\xi = 0$

$$\frac{Kl^3\Delta}{C} = 9\left(\frac{Pl}{C} - 1\right) \tag{45}$$

For $\xi, \eta \neq 0$

$$\frac{Kl^3\Delta}{C} = \frac{Pl}{C} - 1 - 2\frac{K_1}{K}\left(\frac{4\frac{Pl}{C} - 13}{16 - \frac{K_1}{K}}\right) \tag{46}$$

The last three equations are the load shortening relations for the possible equilibrium positions (or modes) and they are subject to the aforementioned limitations on P.

The stability of the column in each of the three modes will now be investigated. The second variation of the potential energy is

$$\delta^2\Pi = \frac{\partial^2\Pi}{\partial\xi^2}(\delta\xi)^2 + 2\frac{\partial^2\Pi}{\partial\xi\,\partial\eta}\delta\xi\,\delta\eta + \frac{\partial^2\Pi}{\partial\eta^2}(\delta\eta)^2$$

For stability in a given equilibrium configuration the second variation must be positive definite in the arbitrary $\delta\xi$ and $\delta\eta$ for this configuration. Thus, for stability both of the coefficients of the squared terms must be positive and the discriminant of the above quadratic form must be negative. If one or both of the coefficients of the squared terms is negative or if the discriminant is positive the equilibrium configuration is unstable.

The ranges of stability are listed below

For $\eta = 0$

$$1 < \frac{Pl}{C} < \left(4\,\frac{K}{K_1} + 3\right) \tag{47}$$

For $\xi = 0$

$$\frac{13}{4} < \frac{Pl}{C} \tag{48}$$

For $\xi, \eta \neq 0$

$$\left(4\,\frac{K}{K_1} + 3\right) < \frac{Pl}{C} < \frac{13}{4} \tag{49}$$

In all other ranges of equilibrium the column is unstable.

Load-shortening curves for the column subject to a controlled load are shown in Figure 3 with the stable and unstable portions indicated. Each set of curves is composed of three straight lines. The line originating at $\frac{Pl}{C} = 1$ (initial buckling load) represents the symmetric equilibrium configuration, the line originating at $\frac{Pl}{C} = 3$ (unstable higher buckling load) represents the antisymmetric equilibrium configuration, and a transition line which extends only between the other two

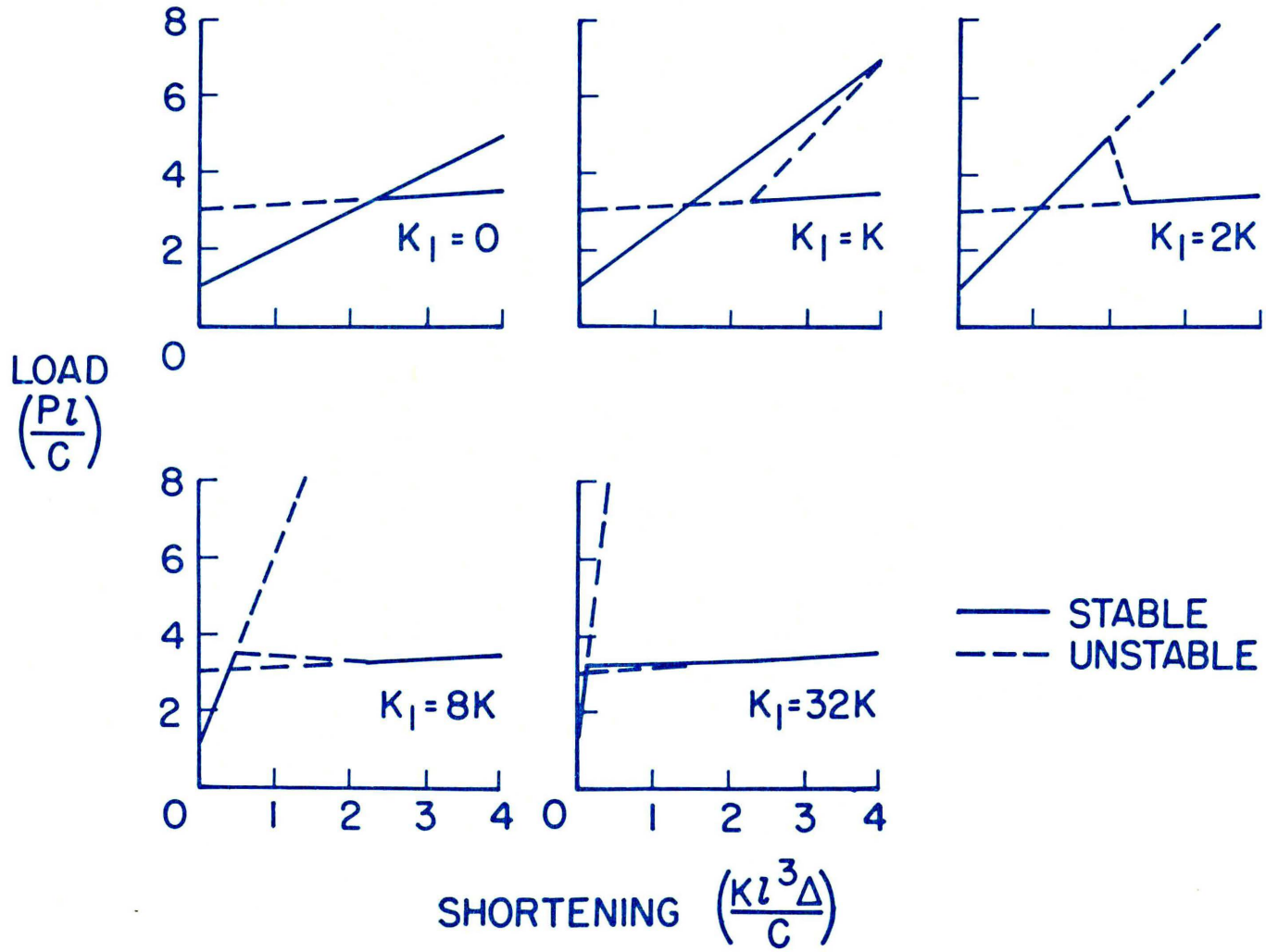

Figure 3.- Load-shortening curves for the three element column. Controlled load.

lines represents the equilibrium configuration which is neither symmetric nor antisymmetric. Each set of curves is for a different ratio of the stiffness of the central to the outside springs. Similar load-shortening curves will be obtained for the column subject to controlled shortening; then both sets of curves will be discussed.

2. Controlled shortening.- For a loading of the type given by a controlled shortening machine the deflections w_1 and w_2 are not arbitrary but are related to the applied shortening Δ. In terms of the variables ξ and η this relationship is

$$l\,\Delta = \xi^2 + 3\eta^2$$

The potential energy for this case is the strain energy. The variable ξ may be eliminated from the strain energy to give

$$\Pi = \frac{K}{2}\left[\left(l\,\Delta - 3\eta^2\right)^2 + 6\left(l\,\Delta - 3\eta^2\right)\eta^2 + \eta^4\right] + \frac{K_1}{4}\left(l\,\Delta - 3\eta^2\right)^2 + \frac{C}{l^2}\left(l\,\Delta + 6\eta^2\right)$$

According to the minimum potential energy method for this case

$$\delta\Pi = \frac{\partial \Pi}{\partial \eta}\,\delta\eta = 0$$

or since the variation of η is arbitrary

$$\frac{\partial \Pi}{\partial \eta} = 0 = \eta\left[-16K\eta^2 - 3K_1\left(l\,\Delta - 3\eta^2\right) + 12\,\frac{C}{l^2}\right]$$

Therefore, either

$$\eta = 0$$

$$\xi^2 = l\,\Delta \qquad (50)$$

or

$$\eta^2 = 3\,\frac{C}{l^2K}\left(\frac{4 - \dfrac{K_1 l^3\Delta}{C}}{16 - 9\,\dfrac{K_1}{K}}\right)$$

$$\xi^2 = l\,\Delta - 9\,\frac{C}{l^2K}\left(\frac{4 - \dfrac{K_1 l^3\Delta}{C}}{16 - 9\,\dfrac{K_1}{K}}\right) \tag{51}$$

Alternatively, by substituting for η instead of ξ in the potential energy, and then varying the potential energy with respect to ξ instead of η, the following additional result is obtained

$$\xi = 0$$

$$\eta^2 = \frac{l\,\Delta}{3} \tag{52}$$

Note that the three cases can be classified, respectively, by $\eta = 0$, $\xi, \eta \neq 0$, and $\xi = 0$.

In order to plot load-shortening curves, as was done for the case of controlled load, use is made of the fact that the derivative of the strain energy with respect to the shortening is equal to the reaction load P. First substitute for ξ and η in the strain energy for each of the three cases. Then differentiation of the strain energy with respect to Δ leads to expressions for P which are identical to those obtained for controlled load. Thus, the equilibrium configurations are the same for both types of load as might be expected. However, the stability of these equilibrium configurations can be different.

The second variation of the potential energy from which ξ has been eliminated is

$$\delta^2\Pi = \frac{\partial^2\Pi}{\partial\eta^2}(\delta\eta)^2$$

Similarly the second variation of the potential energy from which η has been eliminated is

$$\delta^2\Pi = \frac{\partial^2\Pi}{\partial\xi^2}(\delta\xi)^2$$

Since for stability the second variation must be positive, both $\frac{\partial^2\Pi}{\partial\eta^2}$ and $\frac{\partial^2\Pi}{\partial\xi^2}$ (when appropriate) must be positive for the various equilibrium solutions to be stable. Use of these conditions leads to the following ranges of stability:

For $\eta = 0$

$$l\,\Delta < \frac{4C}{l^2K_1} \tag{53}$$

For $\xi = 0$

$$l\,\Delta > \frac{9C}{4l^2K} \tag{54}$$

For $\xi,\eta \neq 0$

$$\frac{9C}{4l^2K} > l\,\Delta > \frac{4C}{l^2K_1} \tag{55}$$

In all other ranges of equilibrium the column is unstable.

Load-shortening curves for both the stable and unstable configurations for the column subject to a controlled shortening are shown in Figure 4. These curves are identical to those obtained for the controlled load case in Figure 3 except that in some ranges the curves of Figure 4 represent stable configurations where in Figure 3 they represented unstable configurations.

B. Results of Simple Model

The results presented in Figures 3 and 4 have some very interesting features. Upon loading the column above the initial buckling load a second buckling load is reached. If, for high values of K_1, either the load or shortening is increased beyond that required for secondary buckling there are continuous stable equilibrium paths available along the transition curve from the symmetric buckling configuration to the antisymmetric buckling configuration. Upon unloading as shown schematically in Figure 5(a), again there are continuous paths available.

For low values of K_1 there are no continuous stable equilibrium paths available. Thus, if either the load or shortening is increased beyond that required for secondary buckling an abrupt change (or jump) will occur as indicated schematically in Figure 5(b) for the case of controlled load. For the case of controlled shortening the jump (when there are no continuous stable paths available) would be at constant shortening. Note that upon unloading as illustrated in Figure 5(b) a different path is followed forming a hysteresis-type loop in the load-shortening curve. The area enclosed in this loop is a measure of the energy expended in the abrupt changes in buckle pattern. Here the system behaves nonconservatively.

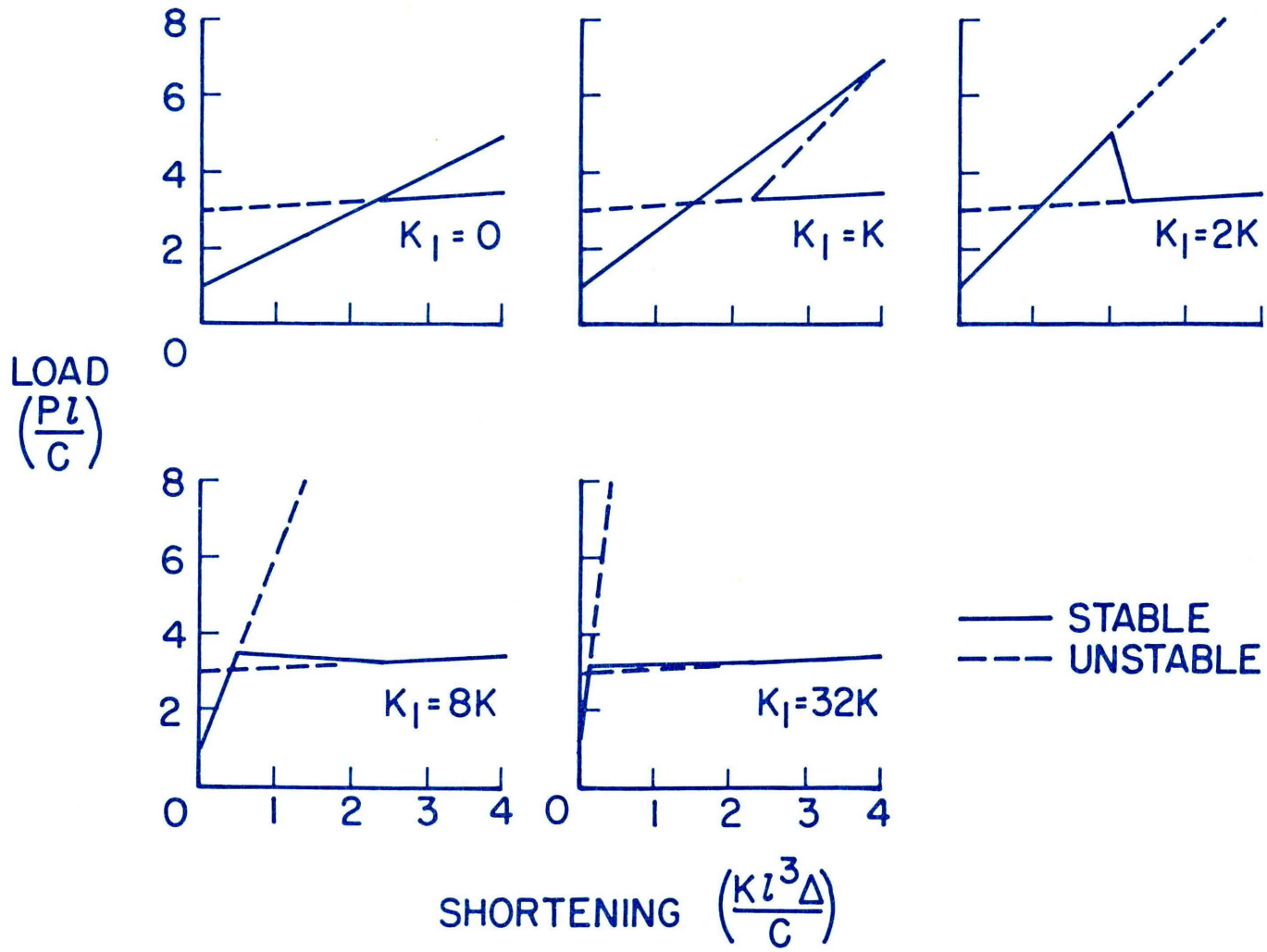

Figure 4.- Load-shortening curves for the three element column. Controlled shortening.

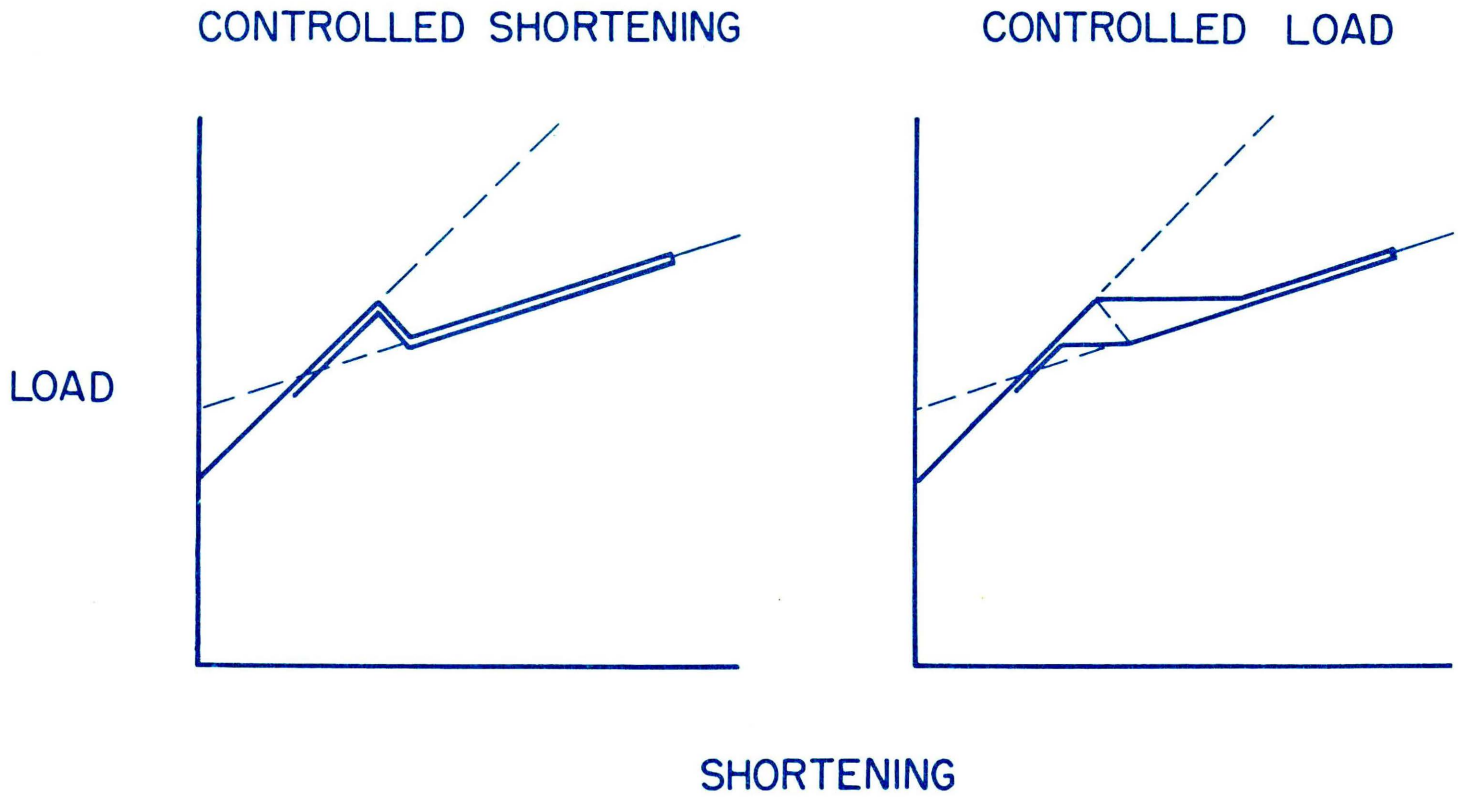

Figure 5.- Schematic diagrams of the loading and unloading of a particular column which has a stable transition for controlled shortening and unstable transition for controlled load.

The results of Figures 3 and 4 show that the load-shortening curves determining equilibrium and the point of secondary buckling are independent of the method of loading, but that some segments of the load-shortening curves are stable or unstable according to the method of loading. Stability occurs as one might expect intuitively. For example, for controlled load, if the transition path from the curve for symmetric buckling to that for antisymmetric buckling indicates increasing load then the transition path is stable - otherwise it is unstable.

Note that the access from the symmetric to the antisymmetric configuration is available only after secondary buckling, and secondary buckling always occurs for loads and shortenings greater than those given by the intersection of the load-shortening curves for the symmetric and antisymmetric equilibrium configurations. Thus, intersections of load-shortening curves for the various equilibrium configurations indicate change in buckle patterns. (This was true in the model analyzed for every case except for the trivial case $K_1 = 0$ where the change in buckle patterns occurred at infinite load.)

Of course, the system under consideration is a conservative one. As long as equilibrium paths are followed the system behaves conservatively. Therefore, the strain energy is equal to the area under the load-shortening curve if equilibrium paths (stable or unstable) are followed. Since the strain energy is path independent, so is the area under the load-shortening curve for equilibrium paths. As a consequence, it can be seen that the area within the triangle to the right of the

intersection of the load-shortening curves for the symmetric and antisymmetric equilibrium configurations is equal to the area within the triangle to the left of this intersection. (See Figs. 3 and 4.)

In order to help visualize what happens during change in buckle pattern, the deflections have been plotted in Figure 6 for one of the columns which has a continuous loading path for controlled shortening as indicated by its load-shortening curve in Figure 4. At the point shortening begins the column buckles into a symmetric configuration ($w_1 = w_2$) as indicated by the solid curve starting from the origin in Figure 6. With increase in shortening the deflections increase until the shortening required for secondary buckling is reached. At this point, with increase in shortening a stable transition configuration is formed which is neither symmetric nor antisymmetric ($w_1 \neq w_2$). Continuing to increase the shortening in this transition range leads to an antisymmetric configuration ($w_1 = -w_2$), and still more increases lead to larger deflections in the antisymmetric configuration. The arrows along the curves in Figure 6 indicate the directions the deflections would take upon loading. The deflections would take the opposite directions for unloading.

C. Extension to Plate Problems

The results just obtained for the three-element column on a nonlinear elastic foundation indicate that intersection between curves for the various equilibrium configuration indicate change in buckle pattern. The load (or shortening) at which change in buckle pattern takes place

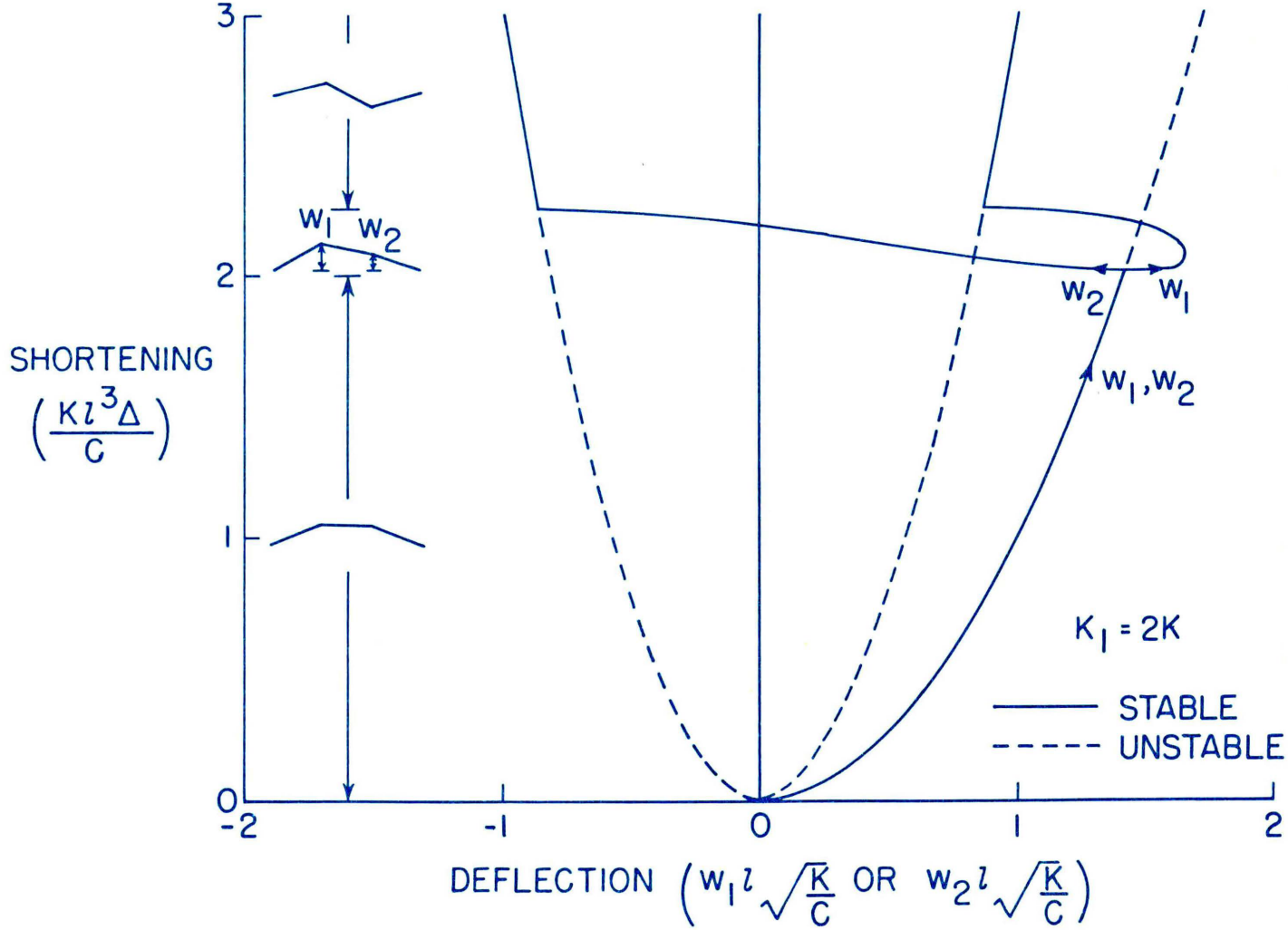

Figure 6.- Equilibrium deflections of a three element column. Controlled shortening.

and the equilibrium paths of loading can be determined from the basic equations. For a conservative system these (continuous) equilibrium paths will lead to the same strain energy regardless of the path of loading. For a system having abrupt changes in buckle pattern hysteresis-type loops in the load-shortening curves can be calculated where the area of the loop will indicate the energy losses. In order to determine the stability of an equilibrium position for the column problem subject to a certain type of loading it was necessary to examine the second variation of the total potential energy. It would be expected that such a procedure would also be necessary for plate problems.

Changes in buckle pattern were not calculated for the plate compression problem because of the extensive calculations required. However, preliminary calculations indicate that for length-width ratios near unity the change in buckle pattern may be of the type given in the column problem for low values of K_1, which implies discontinuous change in buckle pattern for both loadings. On the other hand, for higher length width-ratios, the indications were that the changes would be more like those for higher values of K_1, which imply continuous change in buckle pattern (or at least smaller jumps).

IX. EXPERIMENT

Data are presented from two different kinds of test specimen which will be described in this section. In all the test specimens the loaded edges were ground flat and parallel and perpendicular to the longitudinal axis of the specimen. They were compressed "flat ended" between the platens of the NACA 1,200,000-pound testing machine which applies load through the use of a hydraulic ram.

A. Plate Supported by Multiple-Bay Fixture*

In this test an attempt was made to provide the edge conditions usually specified by theory along the unloaded edges of each panel: simply supported straight edges free of shear.

1. Test specimen.- A 2024-T-3 aluminum alloy flat plate 52.32 × 25.36 × 0.072 was tested.

2. Method of testing.- By supporting the plate laterally with knife edges (on both sides) eleven panels 4.71 × 25.36 were formed. Spur gears attached to the knife edges and racks attached to the fixture base plates were used for positioning knife edges, thus allowing uniform in-plane movement normal to the unloaded edges of each panel. Magnets were installed in the base plate to support the weight of the knife edges during assembly. The knife edges were accurately placed by the use of keys through the base plate which were removed after initial loading. A picture of one of the base plates with the knife edges in place is shown in Figure 7. A lubricant was applied to

*The multiple-bay fixture was designed by Joseph N. Kotanchik and Roger W. Peters of the NACA. The test was conducted by Joseph N. Kotanchik.

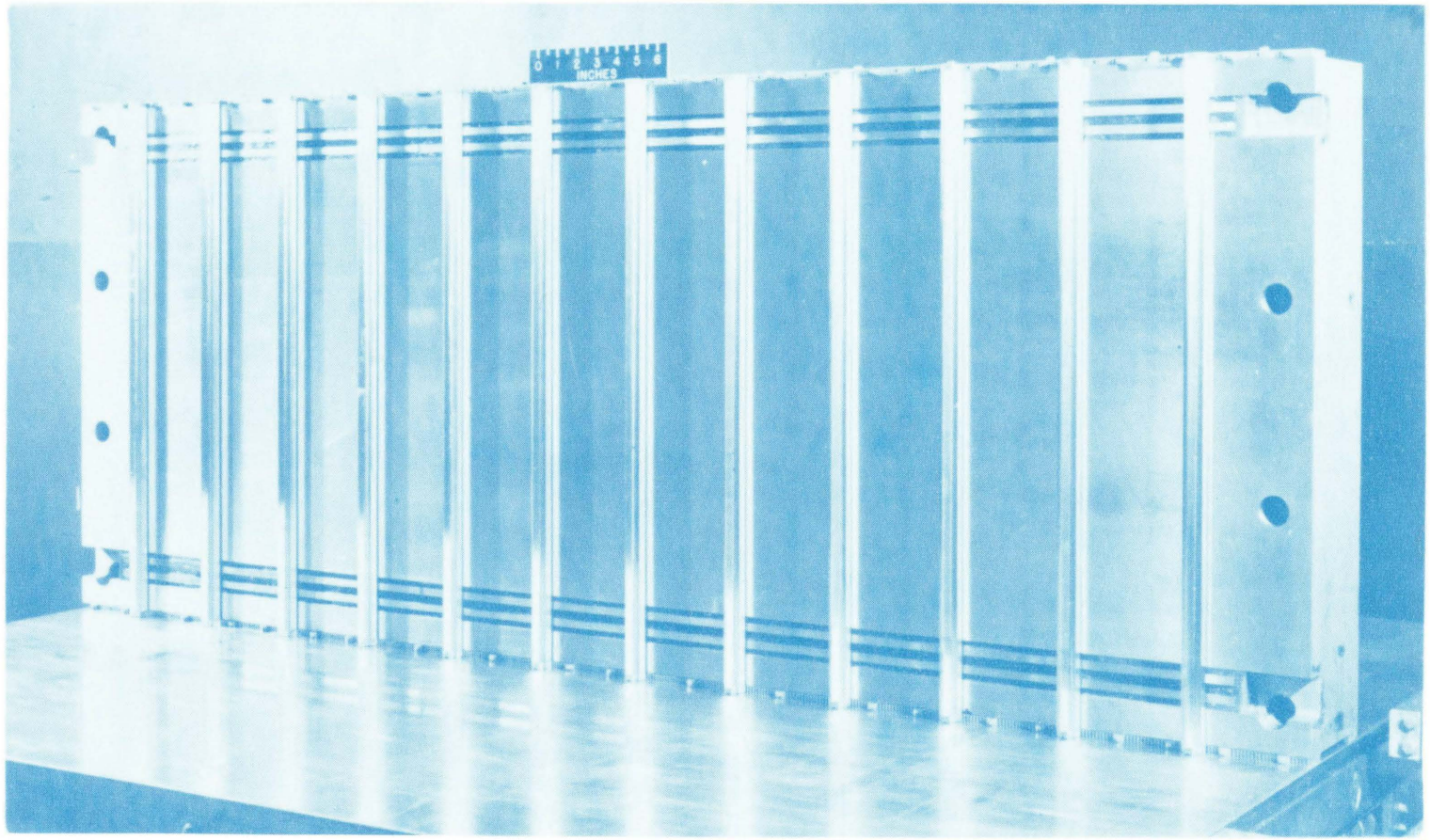

Figure 7.- Base plate of multiple bay fixture showing knife edges used to support flat plate and thus divide plate into eleven panels.

NACA
L-88588

the plate under the knife edges thus permitting in-plane movement of the plate along the unloaded edges leaving them free of shear.

The instrumentation included eight pairs of electric wire strain gages glued to the plate back-to-back and spaced 2 inches apart along the center of the middle bay. The gages were wired so that strain differences could be measured at the location of each pair of gages. Electric wire strain gages on a calibrated cantilever beam were used to measure the total shortening by measuring the change of distance between the platens of the testing machine. The data from all the gages were recorded simultaneously and continuously from initial load to failure.

3. Analysis and discussion of data.- The total shortening data was taken by measuring the distance between the platens at a short distance from the test specimen. Because of deformation of the platens during loading the prebuckling slope of the load-shortening curve was in error. The deformation of the platen is believed to be directly proportional to load, and the data was corrected accordingly. The corrected load-shortening curve is given in nondimensional form in Figure 8. The breaks in the curve after buckling occurred due to changes in buckle pattern. The changes occurred in an explosive manner and were observed to go from 5 to 6 to 7 to 8 buckles.

The pair of back-to-back strain gages along the center line of the middle bay indicating the largest strain difference was assumed to be on the crest of a buckle (no direct observation could be made). No appreciable error is expected from this assumption since there is small variation of strain near the crest of a buckle.

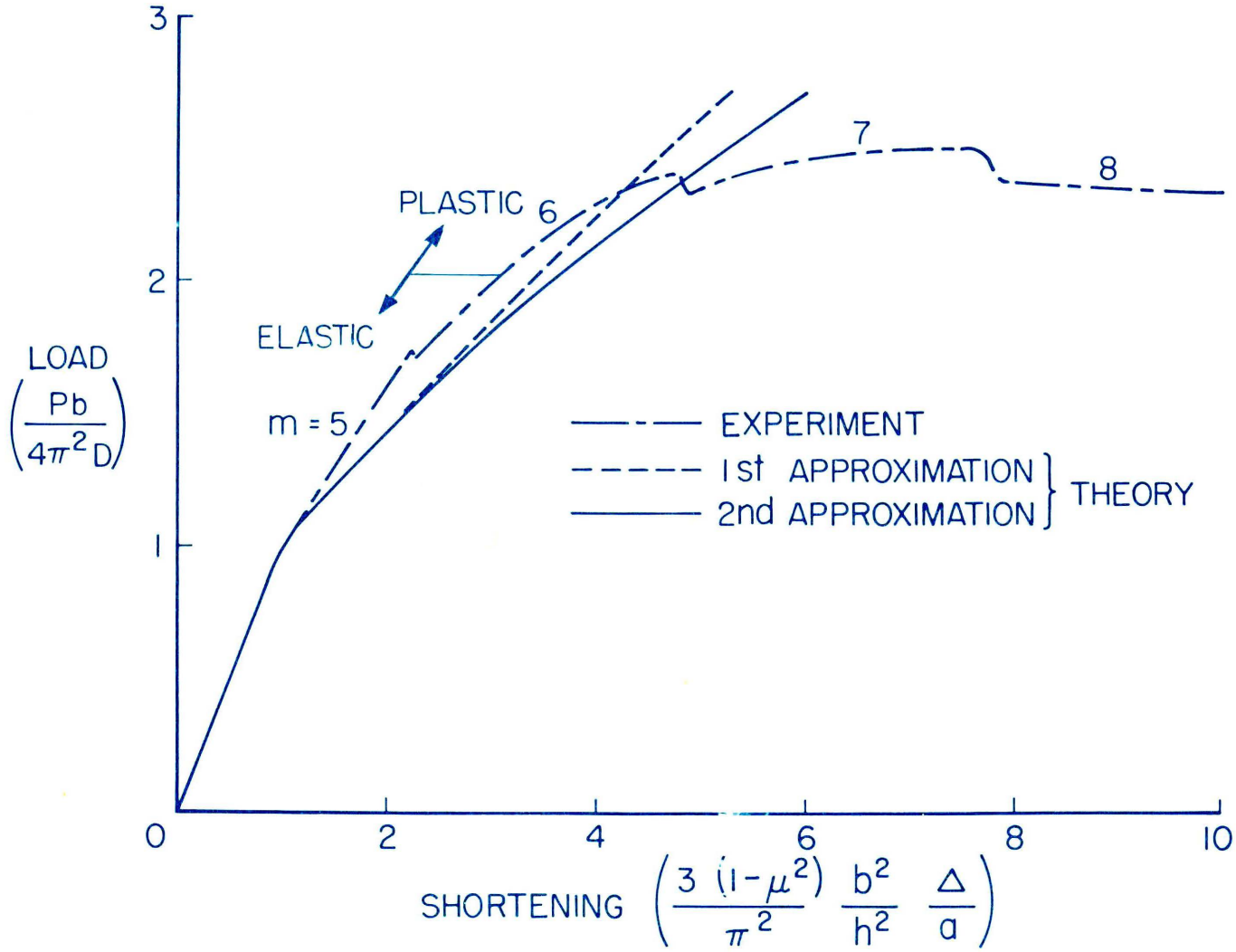

Figure 8.- Comparisons of load-shortening curves as given by (elastic) theory and experiment.

Initially the plate buckled into 5 buckles and one set of gages was nearest the crest. After the buckle pattern change to 6 buckles, another set of gages was nearest the crest. The results from the set of gages nearest the crest in the lower range and the other set of gages in the upper range are shown in nondimensional form in Figure 9 where the bending strain at the crest of the buckle is plotted against the load. The estimated load at which the material became plastic is indicated. The load at which the material started to become plastic was measured by other gages which gave the extreme fiber strains at the crest of the buckle.

B. Z-Stiffened Panels*

Data was obtained in the range from zero strain up to several times the buckling strain on 4 panels similar to those used in aircraft wing construction.

1. Test specimen and instrumentation.- A typical cross section and the important dimensions of the 4 panels tested are shown in Figure 10. Each panel had four Z-section stiffneers attached to flat sheet at three equal spacings. The material in the sheet and stiffeners was artifically aged Alclad aluminum-alloy plate which is discussed in reference 17. Electric wire strain gages were glued to the panels so that strains could be measured at the crest of a buckle and at the stiffeners.

2. Analysis of data.- The strains were measured at intervals of load from initial load to failure. The strains measured at the stiffeners

*These Z-stiffened panels were part of a large group of panels described in reference 17. The panels described here had additional instrumentation in order to be able to study their postbuckling behavior. Joseph N. Kotanchik was in charge of the test program. Many others including the author helped to conduct the tests.

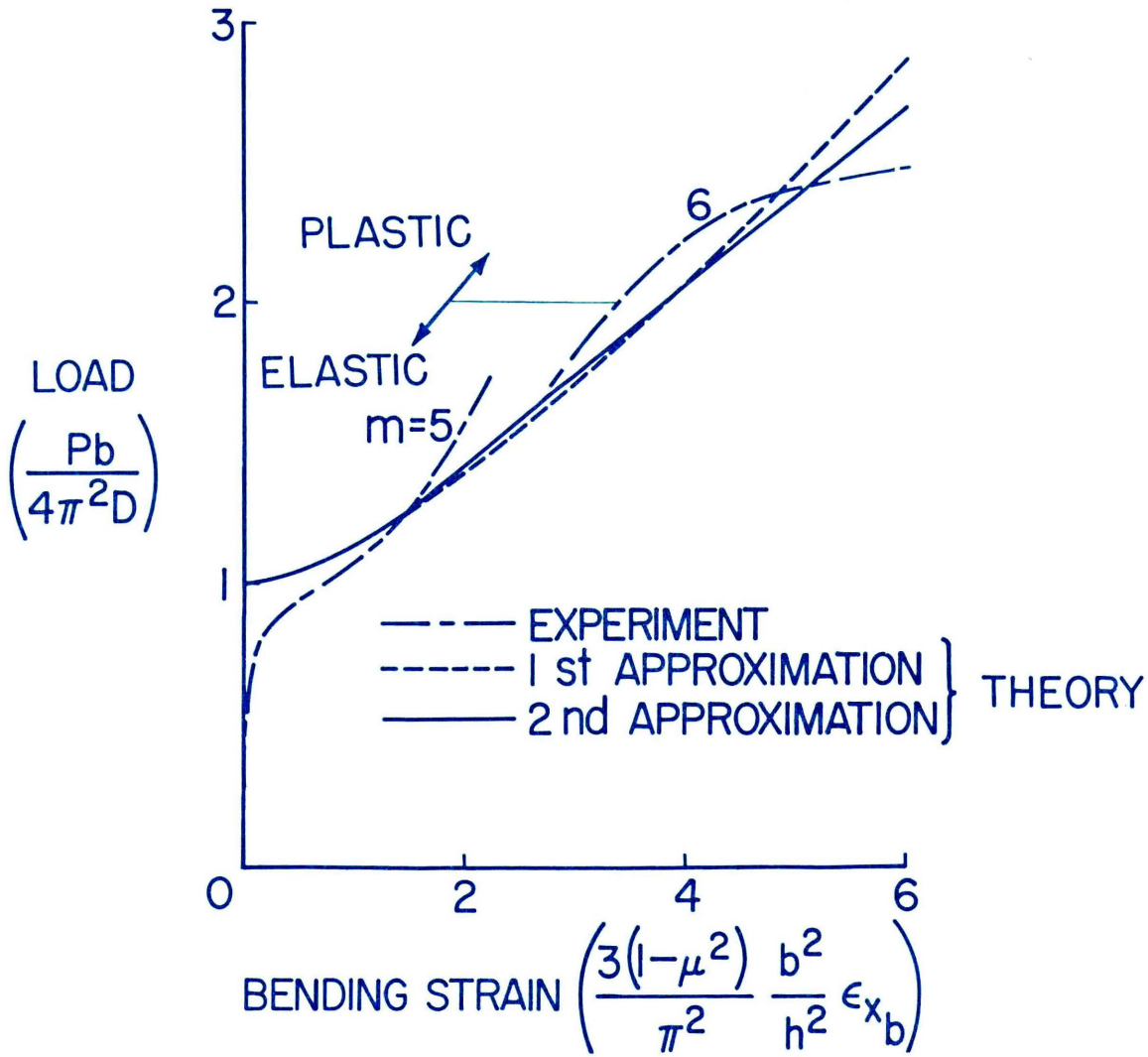

Figure 9.- Comparisons of bending strain at the crest of a buckle as given by (elastic) theory and experiment. ($\mu = 1/3$.)

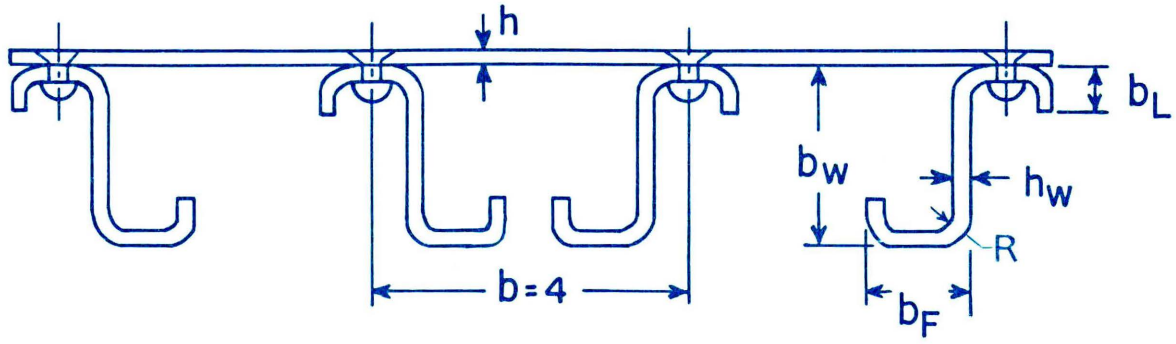

$\frac{b}{h}$	h	a	b_W	h_W	b_F	b_L	R
78.4	0.051	16	$1\frac{1}{2}$	0.091	$\frac{13}{16}$	$\frac{1}{4}$	$\frac{1}{8}$
63.5	.063	16	$1\frac{1}{2}$	.072	$\frac{13}{16}$	$\frac{3}{32}$	$\frac{3}{32}$
48.2	.083	18	2	.091	1	$\frac{3}{8}$	$\frac{1}{8}$
45.5	.088	16	2	.091	1	$\frac{3}{8}$	$\frac{1}{8}$

Figure 10.- A typical cross section and the dimensions of the four Z-stiffened panels tested.

were averaged, and they were plotted against the strain measured at the crest of a buckle in Figure 11. No explosive change in buckle pattern occurred in the range shown. The strains believed to have been in the plastic range are indicated.

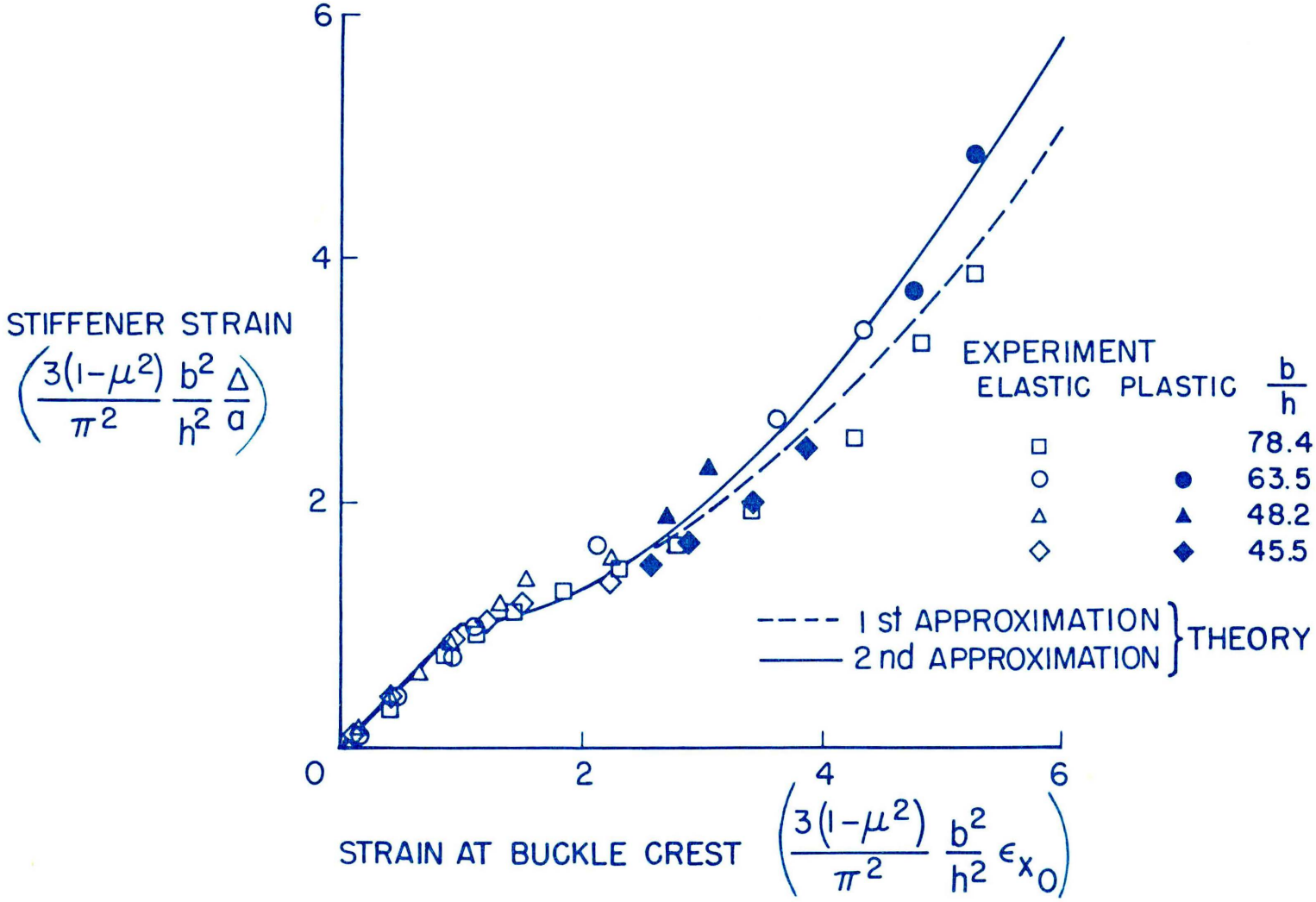

Figure 11.- Comparisons of extreme fiber strains at the crest of a buckle as given by (elastic) theory and experiment. ($\mu = 1/3$.)

X. COMPARISONS OF COMPRESSION THEORETICAL RESULTS WITH OTHER RESULTS

In this section the theoretical results of the example plate compression problem will be compared with the best available previous theoretical results satisfying the same boundary conditions and with experiment.

A. Comparisons With Theory

For the square plate buckling into a square buckle (m = 1) both Levy and Alexeev obtained exact solutions. For a square plate buckling into two buckles (m = 2) Alexeev obtained an exact solution (Levy did not present such a solution). For the range shown in Figure 1, the present results for the second approximation agree with the results of Levy and Alexeev. The results of this dissertation are given in simpler form, and, therefore, should be more useful.

Previous results are available for the initial slope after buckling of plates of various other finite length-width ratios. As can be seen from Figure 1, for some length-width ratios used, these initial slopes would give unduly higher loads for given shortenings everywhere in the postbuckling range except immediately after buckling.

The best available previous results for the infinitely long plates are those of Koiter. The results of the solution of Koiter and the solution of Marguerre follow the curve of the first approximation of the present theory in the first part of the postbuckling range. In the upper part of the range Marguerre's solution continues to follow the first approximation while Koiter's solution follows the dotted line

shown in Figure 12. The results of the second approximation in this dissertation gives lower and hence more accurate loads than previous work.

B. Comparisons With Experiment

The experimental results obtained were for panels subject to "flat end" loading which results in almost complete clamping of the loaded edges. However if the panel tested is long compared to its width (say, of length-width ratio 4 or greater) the size and shape of the buckles near the center will be nearly unaffected by this clamping. Simply supported loaded edges are almost impossible to obtain in the laboratory. The experiments which will be compared to theory here have a length-width ratio of at least 4. Hence, at least certain of the experimental values obtained should be directly comparable to the simply supported theoretical results. As stated in a previous section, the theoretical results for length-width ratio 2 and 4 are not very different from the results for the infinite plate. It would be expected that the theoretical results for any length-width ratio greater than 2 would not be very different from the results for the infinite plate. Thus, the experimental results may be compared to the theoretical results for the infinite plate. Such comparisons are shown in Figures 8, 9, 11, and 13, which will now be discussed in detail.

A comparison with theory is presented in Figure 8 of the experimental load-shortening curve for the test just described of a plate supported by the multiple-bay fixture. The experimental curve shows abrupt changes corresponding to abrupt (explosive) changes in buckle

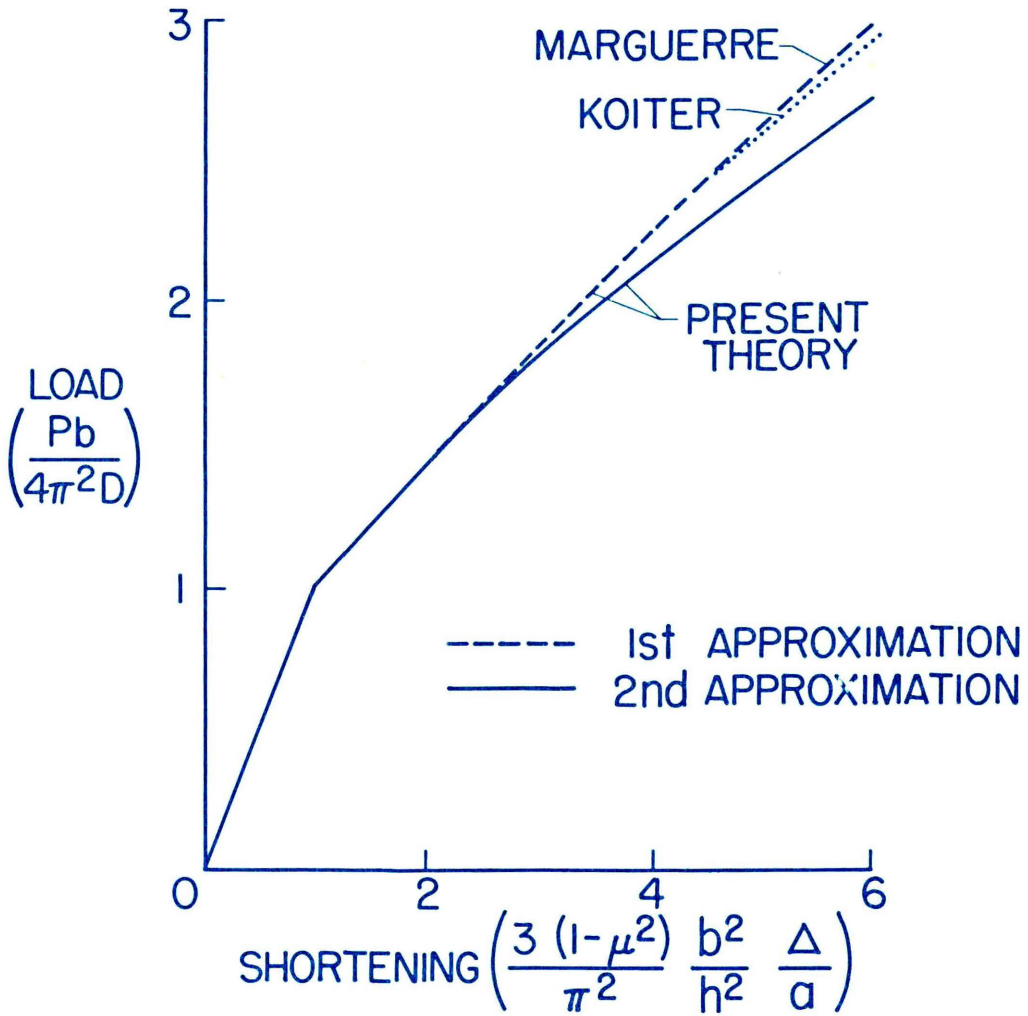

Figure 12.- Comparisons of theoretical load-shortening curves for an infinitely long simply supported plate in longitudinal compression.

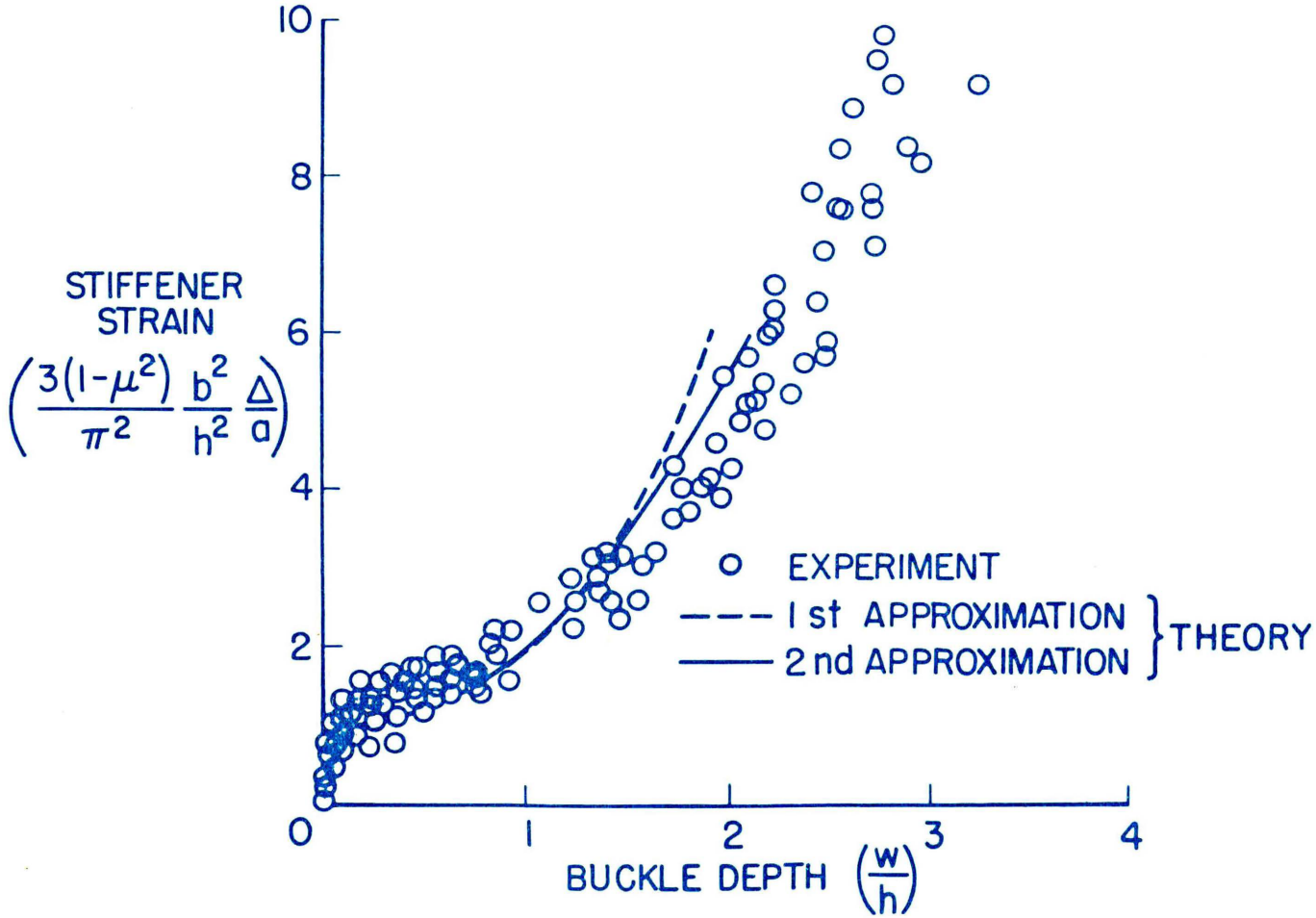

Figure 13.- Comparisons of buckle depth as given by theory and experiment. ($\mu = 1/3$.)

pattern from 5 to 6 to 7 to 8 buckles while the theoretical curve, which is based on continuous change in buckle pattern, is smooth.

Also shown is the load $\left(\frac{Pb}{4\pi^2 D} \approx 2\right)$ when strain gages at the crest of a buckle indicated the plate material had been strained into the plastic range. The type of changes of buckle pattern shown here for a hydraulic-type testing machine by experiment are similar to that described for a controlled-shortening type of loading in the section entitled "The Phenomenon of Change in Buckle Pattern". In consideration of the practical difficulties of measuring total shortening, such as how to account for the bending of the testing machine platens, the present agreement between experiment and theory is good.

Bending strains at the crest of a buckle for the same test are plotted against load and compared to the present theoretical results in Figure 9. Again the abrupt changes in the experimental results do not appear in the theoretical results. The agreement between theory and experiment is good.

In Figure 11 the experimentally measured strains at the crest of the buckle of 4 stiffened panels described in a previous section are plotted against stiffener strain and compared to the present theory. For this set of tests there were no observed changes in the number of buckles from the number which appeared at initial buckling. In the light of previous discussions this is quite surprising. However, it is quite possible that the centrally located buckles could have changed shape as the load progressed. Buckles at the loaded edges could have increased in length while centrally located buckles decreased in length.

Also the edge restraint offered by the stiffener probably decreased as the loading progressed, thus allowing the buckles to become wider. Both of these effects would contribute to smooth and continuous change in buckle pattern similar to that of the infinite plate. From the comparison of the results shown it is evident that although there is scatter at buckling, the theory for simply supported plate gives strains at the crest of the buckle that agree with practical experiment in the postbuckling range.

In Figure 13 buckle depths measured from a series of tests on panels with hat-section stiffeners described in reference 18 are plotted against stiffener strain and are compared to theory. There is a considerable scatter in experimental results. However, it may be stated that in the postbuckling range, theoretical results for the depth of buckle of simply supported plates agree with experimental results on practical stiffened panels.

XI. EXAMPLE TEMPERATURE PROBLEMS

When a simply supported rectangular plate with unrestricted in-plane displacement of its edges is subjected to a uniform temperature rise, the plate simply expands and does not buckle. However, when the in-plane displacement of the edges is restricted, the plate may buckle. Three sets of boundary conditions restricting the in-plane displacement are considered in this section:

(1) Zero displacement normal to the short edges, uniform displacement normal to the long edges, all edges free of shear.

(2) Zero displacement normal to all edges; all edges free of shear.

(3) Zero displacement of all edges.

Except for the third problem the solutions are very similar to that of the compression problem.

The buckling of an infinitely long plate with zero in-plane displacement of all edges subject to a temperature rise is considered separately. The solution of this infinite plate problem is the limiting case for both the second and third problems indicated above.

First the various solutions will be presented in equation form; then curves similar to the load-shortening curves of the compression problem will be presented and discussed. In all the problems the material properties are assumed to be independent of temperature.

A. Solutions

1. Zero displacement normal to the short edges.- With the origin in the corner as for the compression problem the boundary conditions can be written

zero deflection	$w(o,y) = w(a,y) = w(x,o) = w(x,b) = 0$
zero moment	$w_{,xx}(o,y) = w_{,xx}(a,y) = w_{,yy}(x,o) = w_{,yy}(x,b) = 0$
zero displacement	$u(o,y) = u(a,y) = 0$
constant displacement	$v_{,x}(x,o) = v_{,x}(x,b) = 0$
zero shear stress	$v_{,x}(o,y) = v_{,x}(a,y) = u_{,y}(x,o) = u_{,y}(x,b) = 0$
unloaded edges	$\int_o^a (N_y)_{y=o,b}\, dx = 0$

In order to apply these conditions to the set of linear equations (8), insert expressions (5) for u, v, w. It is seen that $u^{(n)}$, $v^{(n)}$, $w^{(n)}$ must individually satisfy the first five lines of boundary conditions. The other condition is equivalent to equations (11). The temperature rise T is taken to be constant and therefore the $T^{(n)}$ are constants.

Solutions of equation (8a) for $u^{(0)}$ and $v^{(0)}$ that satisfy the boundary conditions are

$$u^{(0)} = 0$$

$$v^{(0)} = (1 + \mu)\alpha T^{(0)}\left(y - \frac{b}{2}\right)$$

so that

$$N_x^{(0)} = -Eh\alpha T^{(0)}$$

$$N_y^{(0)} = N_{xy}^{(0)} = 0$$

It can be seen that the solution, except for the following elementary changes, is identical to the solution to the compression problem. For

this solution, however, the parameter ϵ will be related to the temperature rise T as in the following equation (with no loss in generality)

$$\epsilon^2 = \frac{T - T_{cr}}{T_{cr}}$$

where T_{cr} is the temperature rise for buckling which can be identified as equal to $T^{(0)}$ for given values of m and n. It follows that

$$T^{(2)} = T^{(0)} = T_{cr} = \frac{D}{Eh\alpha}$$

and

$$T^{(n)} = 0 \quad \text{for} \quad n \geq 4$$

In order to get the solution to this problem from the solution for the compression problem:

(1) Omit $\left(\frac{x}{a} - \frac{1}{2}\right)$ terms in u.

(2) Change coefficients of $\left(\frac{y}{b} - \frac{1}{2}\right)$ terms in v.

(a) Replace $-\mu \frac{Pb}{4\pi^2 D}$ by $\frac{3(1+\mu)(1-\mu^2)}{\pi^2} \frac{b^2}{h^2} \alpha T$

(b) Replace $\frac{\delta^2 n^2}{2}$ by $\frac{\delta^2}{2}(n^2 + \mu\beta^2)$

(c) Replace $\delta^4 \bar{w}_3 n^2$ by $\delta^4 \bar{w}_3 (n^2 + \mu\beta^2)$

(3) Replace $-\frac{P}{b}$ term in N_x by $-\frac{D\pi^2}{b^2}\left(\frac{12(1-\mu^2)}{\pi^2} \frac{b^2}{h^2} \alpha T - 2\beta^2\delta^2 - 4\beta^2\delta^4 \bar{w}_3\right)$

(4) Redefine
$$\begin{cases} \delta^2 = \dfrac{\dfrac{12(1-\mu^2)}{\pi^2}\dfrac{b^2}{h^2}\alpha T\beta^2 - (\beta^2+n^2)^2}{3\beta^4+n^4} \\ \bar{w}_1 = \dfrac{3}{2}\dfrac{\beta^4 \bar{w}_{13}^{(3)} + n^4 \bar{w}_{31}^{(3)}}{3\beta^4+n^4} \end{cases}$$

2. Zero displacement normal to all edges.- With the origin in the corner as in the previous problems the boundary condition can be written

zero deflection $\quad w(o,y) = w(a,y) = w(x,o) = w(x,b) = 0$

zero moment $\quad w_{,xx}(o,y) = w_{,xx}(a,y) = w_{,yy}(x,o) = w_{,yy}(x,b) = 0$

zero displacement $\quad u(o,y) = u(a,y) = v(x,o) = v(x,b) = 0$

zero shear stress $\quad v_{,x}(o,y) = v_{,x}(a,y) = u_{,y}(x,o) = u_{,y}(x,b) = 0$

The above conditions must hold for the values $u^{(n)}$, $v^{(n)}$, $w^{(n)}$, also. Again the $T^{(n)}$ are constant.

Solutions of equations (8a) that satisfy boundary conditions are $u^{(0)} = v^{(0)} = 0$ so that

$$N_x^{(0)} = N_y^{(0)} = -\frac{Eh}{1-\mu}\alpha T^{(0)}$$

$$N_{xy}^{(0)} = 0$$

Again it can be seen that the solution except for some elementary changes is identical to the solution for the compression problem.

As in the previous temperature problem, let

$$\epsilon^2 = \frac{T - T_{cr}}{T_{cr}}$$

and it follows that

$$T^{(2)} = T^{(0)} = T_{cr} = \frac{D(1-\mu)}{Eha}\left[\left(\frac{m\pi}{a}\right)^2 + \left(\frac{n\pi}{b}\right)^2\right]$$

$$T^{(n)} = 0 \quad \text{for} \quad n \geq 4$$

In order to get the solution to this problem from the compression problem:

(1) Omit $\left(\frac{x}{a} - \frac{1}{2}\right)$ terms in u.

(2) Omit $\left(\frac{y}{b} - \frac{1}{2}\right)$ terms in v.

(3) Replace $-\frac{P}{b}$ term in N_x by

$$-\frac{D\pi^2}{b^2}\left(\frac{12(1+\mu)}{\pi^2}\frac{b^2}{n^2}\alpha T - 2\delta^2\frac{\beta^2+\mu n^2}{1-\mu^2} - 4\delta^4\frac{\beta^2+\mu n^2}{1-\mu^2}\bar{w}_z\right)$$

(4) Insert following term in N_y:

$$-\frac{D\pi^2}{b^2}\left(\frac{12(1+\mu)}{\pi^2}\frac{b^2}{h^2}\alpha T - 2\delta^2\frac{n^2+\mu\beta^2}{1-\mu^2} - 4\delta^4\frac{n^2+\mu\beta^2}{1-\mu^2}\bar{w}_z\right)$$

(5) Redefine

$$\delta^2 = (1-\mu^2)\frac{\frac{12(1+\mu)}{\pi^2}\frac{b^2}{h^2}\alpha T(\beta^2+n^2) - (\beta^2+n^2)^2}{(3-\mu^2)(\beta^4+n^4) + 4\mu\beta^2n^2}$$

$$\bar{w}_{13}^{(3)} = \frac{\beta^4}{8n^2(\beta^2+9n^2)}$$

$$\bar{w}_3 = \frac{3}{2}(1-\mu^2)\frac{\beta^4\bar{w}_{13}^{(3)} + n^4\bar{w}_{31}^{(3)}}{(3-\mu^2)(\beta^4+n^4) + 4\mu\beta^2n^2}$$

$$\bar{w}_{31}^{(3)} = \frac{n^4}{8\beta^2(9\beta^2+n^2)}$$

3. Zero displacement of all edges.- With the origin in the corner as in the previous problems the boundary conditions can be written

zero deflection $\quad w(o,y) = w(a,y) = w(x,o) = w(x,b) = 0$

zero moment $\quad w_{,xx}(o,y) = w_{,xx}(a,y) = w_{,yy}(x,o) = w_{,yy}(x,b) = 0$

zero displacement $\quad u = v = 0$ on all edges

The above equations must hold for the values $u^{(n)}$, $v^{(n)}$, $w^{(n)}$ also. Again the $T^{(n)}$ are constant.

Solutions of equations (8a) that satisfy boundary conditions are $u^{(0)} = v^{(0)} = 0$ so that

$$N_x^{(0)} = N_y^{(0)} = \frac{Eh\alpha T^{(0)}}{1-\mu}$$

$$N_{xy}^{(0)} = 0$$

The solutions for $w^{(1)}$ and $T^{(0)}$ are identical in form to the previous case

$$w^{(1)} = w_1 \sin\frac{m\pi x}{a}\sin\frac{n\pi y}{b}$$

$$T^{(0)} = \frac{D(1-\mu)}{Eh\alpha}\left[\left(\frac{m\pi}{a}\right)^2 + \left(\frac{n\pi}{b}\right)^2\right]$$

The solutions for $u^{(2)}$ and $v^{(2)}$ are not obtainable as easily as in the previous cases because the boundary conditions for this case cannot be satisfied by a few simple trigonometric expressions. If the solution is taken in the form

$$u^{(2)} = \frac{w_1^2}{8}\left[U(x,y) + \frac{1}{2}\frac{m\pi}{a}\sin\frac{2m\pi x}{a}\left(\cos\frac{2n\pi y}{b} - 1\right)\right]$$

$$v^{(2)} = \frac{w_1^2}{8}\left[V(x,y) + \frac{1}{2}\frac{n\pi}{b}\left(\cos\frac{2m\pi x}{a} - 1\right)\sin\frac{2n\pi y}{b}\right]$$

the equation giving U and V which are obtained from equations (8c) are

$$U_{,xx} + \frac{1-\mu}{2}U_{,yy} + \frac{1+\mu}{2}V_{,xy} = -2\mu\frac{m\pi}{a}\left(\frac{n\pi}{b}\right)^2\sin\frac{2m\pi x}{a}$$

$$\frac{1+\mu}{2}U_{,xy} + V_{,yy} + \frac{1-\mu}{2}V_{,xx} = -2\mu\frac{n\pi}{b}\left(\frac{m\pi}{a}\right)^2\sin\frac{2n\pi y}{b}$$

with the boundary conditions that $U = V = 0$ on all edges. In addition U is antisymmetric in the x direction and symmetric in the y direction and V is antisymmetric in the y direction and symmetric in the x direction. Fourier series which satisfy boundary and symmetry conditions term by term for the unknown U and V are

$$U = \sum_{i=2,4}^{\infty}\sum_{j=1,3}^{\infty} a_{ij}\sin\frac{i\pi x}{a}\sin\frac{j\pi y}{b}$$

$$V = \sum_{i=1,3}^{\infty} \sum_{j=2,4}^{\infty} b_{ij} \sin \frac{i\pi x}{a} \sin \frac{j\pi y}{b}$$

Using these series for U and V in conjunction with the Galerkin method leads to the following pair of linear algebraic equations which determine a_{ij} and b_{ij}

$$a_{rs}\left[\left(\frac{rb}{a}\right)^2 + \frac{1-\mu}{2} s^2\right] - \frac{8(1+\mu)}{\pi^2} \frac{b}{a} \sum_{i=1,3}^{\infty} \sum_{j=2,4}^{\infty} b_{ij} \frac{ijrs}{(r^2 - i^2)(s^2 - j^2)} =$$

$$\frac{8\mu}{a} \frac{mn^2}{s} \delta_{r,2m} \qquad (r = 2,4,\ldots \qquad s = 1,3,\ldots)$$

$$b_{rs}\left[s^2 + \frac{1-\mu}{2}\left(\frac{rb}{a}\right)^2\right] - \frac{8(1+\mu)}{\pi^2} \frac{b}{a} \sum_{i=2,4}^{\infty} \sum_{j=1,3}^{\infty} a_{ij} \frac{ijrs}{(r^2 - i^2)(s^2 - j^2)} =$$

$$\frac{8\mu}{a} \frac{nm^2}{r} \frac{b}{a} \delta_{s,2n} \qquad (r = 1,3,\ldots \qquad s = 2,4,..)$$

where the δ's are the Kroneker deltas which are defined to vanish if the subscripts are different and to equal unity if the subscripts are the same. The number of different a_{ij} and b_{ij} required for convergence will depend on the buckle configuration considered.

If, for example, the square plate that has buckled into one buckle is considered $\left(m = n = \frac{a}{b} = 1\right)$, the following values for the most important a_{ij} and b_{ij} are obtained

$$a_{21} = b_{12} = 0.2202(8\mu/a)$$

$$a_{23} = b_{32} = 0.0595(8\mu/a)$$

$$a_{25} = b_{52} = 0.0187(8\mu/a)$$

$$a_{27} = b_{72} = 0.0086(8\mu/a)$$

Once the a_{ij} and b_{ij} are found, the solution may be continued

$$N_x^{(2)} + N_x^{(11)} = -\frac{Eh\alpha T^{(2)}}{1-\mu} + \frac{Eh}{1-\mu^2}\frac{w_1^2}{8}\left[\left(\frac{m\pi}{a}\right)^2\left(1 - \cos\frac{2n\pi y}{b}\right) + \mu\left(\frac{n\pi}{b}\right)^2\left(1 - \cos\frac{2m\pi x}{a}\right) + U_{,x} + \mu V_{,y}\right]$$

$$N_y^{(2)} + N_y^{(11)} = -\frac{Eh\alpha T^{(2)}}{1-\mu} + \frac{Eh}{1-\mu^2}\frac{w_1^2}{8}\left[\left(\frac{n\pi}{b}\right)^2\left(1 - \cos\frac{2m\pi x}{a}\right) + \mu\left(\frac{m\pi}{a}\right)^2\left(1 - \cos\frac{2n\pi y}{b}\right) + V_{,y} + \mu U_{,x}\right]$$

$$N_{xy}^{(2)} + N_{xy}^{(11)} = \frac{Eh}{2(1+\mu)}\frac{w_1^2}{8}(U_{,y} + V_{,x})$$

and w_1 may be obtained from

$$\int_0^b\int_0^a\left[\left(N_x^{(2)} + N_x^{(11)}\right)w_{,xx}^{(1)} + \left(N_y^{(2)} + N_y^{(11)}\right)w_{,yy}^{(1)} + 2\left(N_{xy}^{(2)} + N_{xy}^{(11)}\right)w_{,xy}^{(1)}\right]\sin\frac{m\pi x}{a}\sin\frac{n\pi y}{b}\,dx\,dy = 0$$

The solution for w_1 is given below in terms of the a_{ij} and b_{ij}

$$w_1^2 = 16(1+\mu)\alpha T^{(2)}\left[\left(\frac{m\pi}{a}\right)^2 + \left(\frac{n\pi}{b}\right)^2\right] \div \left\{3\left(\frac{m\pi}{a}\right)^4 + 2\mu\,\frac{m\pi}{a}\,\frac{n\pi}{b} + \left(\frac{n\pi}{b}\right)^4 - \frac{4m}{a}\left[\left(\frac{m\pi}{a}\right)^2 + \mu\left(\frac{n\pi}{b}\right)^2\right]\sum_{j=1,3}^{\infty} a_{2m,j}\,\frac{1}{j} - \frac{4n}{b}\left[\left(\frac{n\pi}{b}\right)^2 + \mu\left(\frac{m\pi}{a}\right)^2\right]\sum_{i=1,3}^{\infty} b_{i,2n}\,\frac{1}{i} + \left[\left(\frac{m\pi}{a}\right)^2 + \left(\frac{n\pi}{b}\right)^2\right]\left(\frac{4m}{a}\sum_{j=1,3}^{\infty}\frac{j a_{2m,j}}{j^2 - 4m^2} + \frac{4n}{b}\sum_{i=1,3}^{\infty}\frac{i b_{i,2n}}{i^2 - 4n^2}\right)\right\}$$

The first approximation may now be written if values are assigned to the perturbation parameter ϵ. The solution for this problem is not carried beyond the first approximation because of the complexity of the analysis.

As in the other temperature problems, there is no loss in generality if

$$\epsilon^2 = \frac{T - T_{cr}}{T_{cr}}$$

and it follows that

$$T^{(2)} = T^{(0)} = T_{cr}$$

$$T^{(n)} = 0 \quad \text{for} \quad n \geq 4$$

In the following, results for the deflections and stresses are written in equation form for the first approximation

$$u = \frac{\pi^2}{3(1-\mu^2)} \frac{h^2 a}{b^2} \delta^2 \left[\frac{\beta^2}{4m\pi} \sin \frac{2m\pi x}{a} \left(\cos \frac{2n\pi y}{b} - 1 \right) + \frac{1}{2} \frac{b^2}{a\pi^2} \sum_{i=2,4}^{\infty} \sum_{j=1,3}^{\infty} a_{ij} \sin \frac{i\pi x}{a} \sin \frac{j\pi y}{b} \right]$$

$$v = \frac{\pi^2}{3(1-\mu^2)} \frac{h^2}{b} \delta^2 \left[\frac{n}{4\pi} \left(\cos \frac{2m\pi x}{a} - 1 \right) \sin \frac{2n\pi y}{b} + \frac{1}{2} \frac{b}{\pi^2} \sum_{i=1,3}^{\infty} \sum_{j=2,4}^{\infty} b_{ij} \sin \frac{i\pi x}{a} \sin \frac{j\pi y}{b} \right]$$

$$w = \frac{2h\delta}{\sqrt{3(1-\mu^2)}} \sin\frac{m\pi x}{a} \sin\frac{n\pi y}{b}$$

$$N_x = \frac{D\pi^2}{b^2}\left\{-\frac{12(1+\mu)}{\pi^2}\frac{b^2}{h^2}\alpha T + \frac{2\delta^2}{1-\mu^2}\left[\beta^2\left(1-\cos\frac{2n\pi y}{b}\right) + \mu n^2\left(1-\cos\frac{2m\pi x}{a}\right) + \frac{b^2}{a\pi}\sum_{i=2,4}^{\infty}\sum_{j=1,3}^{\infty} ia_{ij}\cos\frac{i\pi x}{a}\sin\frac{j\pi y}{b} + \mu\frac{b}{\pi}\sum_{i=1,3}^{\infty}\sum_{j=2,4}^{\infty} jb_{ij}\sin\frac{i\pi x}{a}\cos\frac{j\pi y}{b}\right]\right\}$$

$$N_y = \frac{D\pi^2}{b^2}\left\{-\frac{12(1+\mu)}{\pi^2}\frac{b^2}{h^2}\alpha T + \frac{2\delta^2}{1-\mu^2}\left[n^2\left(1-\cos\frac{2m\pi x}{a}\right) + \mu\beta^2\left(1-\cos\frac{2n\pi y}{b}\right) + \frac{b}{\pi}\sum_{i=1,3}^{\infty}\sum_{j=2,4}^{\infty} jb_{ij}\sin\frac{i\pi x}{a}\cos\frac{j\pi y}{b} + \mu\frac{b^2}{a\pi}\sum_{i=2,4}^{\infty}\sum_{j=1,3}^{\infty} ia_{ij}\cos\frac{i\pi x}{a}\sin\frac{j\pi y}{b}\right]\right\}$$

$$N_{xy} = \frac{D\pi^2}{b^2}\frac{\delta^2}{1+\mu}\left(\frac{b}{\pi}\sum_{i=2,4}^{\infty}\sum_{j=1,3}^{\infty} ja_{ij}\sin\frac{i\pi x}{a}\cos\frac{j\pi y}{b} + \frac{b^2}{a\pi}\sum_{i=1,3}^{\infty}\sum_{j=2,4}^{\infty} ib_{ij}\cos\frac{i\pi x}{a}\sin\frac{j\pi y}{b}\right)$$

where here

$$\delta^2 = (1 - \mu^2)\left[\frac{12(1 + \mu)}{\pi^2}\frac{b^2}{h^2}\alpha T(\beta^2 + n^2) - (\beta^2 + n^2)^2\right] \div$$

$$\left[3(\beta^4 + 2\mu\beta^2 n^2 + n^4) - 4\beta(\beta^2 + \mu n^2)\frac{b}{\pi^2}\sum_{j=1,3}^{\infty} a_{2m,j}\frac{1}{j} - \right.$$

$$4n(n^2 + \mu\beta^2)\frac{b}{\pi^2}\sum_{i=1,3}^{\infty} b_{i,2n}\frac{1}{i} + (\beta^2 + n^2)\left(4\beta\frac{b}{\pi^2}\sum_{j=1,3}^{\infty} a_{2m,j}\frac{j}{j^2 - 4n^2} + \right.$$

$$\left.\left. 4n\frac{b}{\pi^2}\sum_{i=1,3}^{\infty}\frac{i}{i^2 - 4n^2}\right)\right]$$

4. Infinitely long plate with zero displacement of all edges.- The problem solved is the postbuckling behavior of a simply supported infinitely long plate with zero in-plane displacement of all edges subject to a uniform temperature rise. Only the buckle pattern with one buckle in the long direction (cylindrical buckling) will be examined in this section. Cylindrical buckling occurs for the lowest buckling load, and as discussed later in this appendix no change in buckle pattern is indicated.

For this case the deflection normal to the plate w and the displacement v may be considered to be functions of y only and the displacement u is zero everywhere. With the origin along the lower edge of an infinite plate of width b, the remaining boundary conditions may be written

zero deflection $\quad w(o) = w(b) = 0$

zero moment $\quad w_{,yy}(o) = w_{,yy}(b) = 0$

zero displacement $\quad v(o) = v(b) = 0$

In order to apply these conditions to the derived equations, insert expressions (5) for v and w. It is seen that $v^{(n)}$ and $w^{(n)}$ must individually satisfy these conditions. Again the temperature rise is uniform and therefore the $T^{(n)}$ are constant.

Solution of equation (8a) that satisfies the boundary condition is (u = 0)

$$v^{(0)} = 0$$

so that

$$N_x^{(0)} = N_y^{(0)} = -\frac{Eh}{1-\mu}\alpha T^{(0)}$$

$$N_{xy}^{(0)} = 0$$

For this problem equation (8b) has the solution

$$w^{(1)} = w_1 \sin\frac{n\pi y}{b}$$

that satisfies the boundary conditions. This solution requires that

$$T^{(0)} = \frac{D(1-\mu)}{Eh\alpha}\left(\frac{n\pi}{b}\right)^2$$

So far the solutions obtained are identical to the small deflection solutions where the set of values of $T^{(0)}$ (for each n) can be identified as the set of temperature rises that would cause buckling.

The lowest temperature rise that would cause buckling is the one corresponding to $n = 1$. Note that, as in small deflection theory, the amplitude w_1 cannot be determined (as yet).

The $N^{(11)}$'s may be found now (in terms of w_1), and from equation (8c) the solution that satisfies the boundary conditions is

$$v^{(2)} = -\frac{w_1^2}{8}\frac{n\pi}{b}\sin\frac{2n\pi y}{b}$$

so that

$$N_x^{(2)} + N_x^{(11)} = \frac{Eh}{1-\mu^2}\left[-(1+\mu)\alpha T^{(2)} + \mu\frac{w_1^2}{4}\left(\frac{n\pi}{b}\right)^2\right]$$

$$N_y^{(2)} + N_y^{(11)} = \frac{Eh}{1-\mu^2}\left[-(1+\mu)\alpha T^{(2)} + \frac{w_1^2}{4}\left(\frac{n\pi}{b}\right)^2\right]$$

$$N_{xy}^{(2)} + N_{xy}^{(11)} = 0$$

Now $w^{(3)}$ must be determined from equation (8d). After substitution for the N's and $w^{(1)}$, equation (8d) becomes ($w^{(3)}$ is a function of y only)

$$Dw^{(3)}_{,yyyy} + \frac{Eh}{1-\mu}\alpha T^{(0)}w^{(3)}_{,yy} = \frac{Eh}{1-\mu^2}\left(\frac{n\pi}{b}\right)^2\left[-(1+\mu)\alpha T^{(2)} + \frac{w_1^2}{4}\left(\frac{n\pi}{b}\right)^2\right]\sin\frac{n\pi y}{b}$$

In order that this equation has a solution satisfying boundary conditions

$$w_1^2 = \frac{4(1+\mu)\alpha T^{(2)}}{\left(\frac{n\pi}{b}\right)^2}$$

If at this point the arbitrary parameter ϵ^2 is assigned the value $\frac{T - T_{cr}}{T_{cr}}$. It follows that

$$T^{(2)} = T^{(0)} = T_{cr}$$

$$T^{(n)} = 0 \quad \text{for} \quad n \geq 4$$

It can be seen now that there is no contribution of any other of the set of equations (8). Therefore, an exact solution has been obtained for this problem. The final results can be written

$$u = 0$$

$$v = -\left(T - \frac{D(1 - \mu)\left(\frac{n\pi}{b}\right)^2}{Eh\alpha}\right)\frac{(1 + \mu)\alpha}{\frac{2n\pi}{b}} \sin \frac{2n\pi y}{b}$$

$$w = \sqrt{(1 + \mu)\alpha\left(T - \frac{D(1 - \mu)\left(\frac{n\pi}{b}\right)^2}{Eh\alpha}\right)}\frac{2b}{n\pi} \sin \frac{n\pi y}{b}$$

$$N_x = -Eh\alpha T - \mu D\left(\frac{n\pi}{b}\right)^2$$

$$N_y = -D\left(\frac{n\pi}{b}\right)^2$$

$$N_{xy} = 0$$

It may be noted that N_y remains at the buckling value in the postbuckling range.

B. Curves

For the temperature problems it is desirable to have curves similar to the load-shortening curves of the compression problem. The particular advantage of the load-shortening curve is that the area under the curve is equal to the strain energy. Thus there is a convenient indication of the possibility of change in buckle pattern. For the temperature problems considered there does not exist a strain energy as such. However, there does exist a comparable quantity, the energy (at the final temperature) which is released when the edge restraints are removed (reversibly). This "recoverable" energy is equal to the strain energy of a slightly larger simply supported plate with edges subjected to loads equal to the reaction loads at the in-plane restraints.

The recoverable strain energy will now be examined. If the reaction loads at the restraints are N_x, N_y, N_{xy}, and the displacements that occur upon relaxing the restraints are $\bar{u}$ and $\bar{v}$ then the recoverable strain energy U is

$$U = \int_0^\tau \left[\int_0^b \left(N_x \frac{\partial \bar{u}}{\partial t} \right)_{x=a} dy + \int_0^a \left(N_y \frac{\partial \bar{v}}{\partial t} \right)_{y=b} dx + \right.$$

$$\left. \int_0^b \left(N_{xy} \frac{\partial \bar{v}}{\partial t} \right)_{x=a} dy + \int_0^a \left(N_{xy} \frac{\partial \bar{u}}{\partial t} \right)_{y=b} dx \right] dt$$

where at $t = 0$ the plate is unloaded and at $t = \tau$ the plate is loaded. Since the final values of $\bar{u}$ and $\bar{v}$ at the boundaries are functions of the temperature rise T and since the reaction loads are

given in the analysis section as function of the temperature rise T, it is convenient to change the variable of integration from t to T. This may be done since the strain energy is independent of path. The recoverable strain energy will now be discussed in more detail for each of the temperature problems.

For the first problem the N_y and N_{xy} terms will not appear, and since $\bar{u}$ is not a function of y at $x = a$

$$U = -\int_0^T P\left(\frac{\partial \bar{u}}{\partial t}\right)_{x=a} dt$$

where

$$P = -\int_0^b (N_x)_{x=a} dy$$

As $t = 0$, $\bar{u}(a,y) = a\alpha T$ and at $t = \tau$, $\bar{u}(a,y) = 0$ so that by changing the variable of integration the above expression for energy can be written

$$U = \int_0^{a\alpha T} P\, d(\bar{u})_{x=a}$$

Changing the variable of integration again gives

$$U = a\alpha \int_0^T P\, dT$$

Therefore, if P is plotted against $a\alpha T$ or if $\partial U/\partial t$ is plotted against T the area under the curve up to the temperature rise T in question will be equal to the recoverable strain energy. Obviously for this problem $\partial U/\partial t = a\alpha P$.

For the second problem (simply supported plate subject to uniform temperature rise with zero displacement normal to all edges, zero shear on all edges) the N_{xy} terms disappear and $\bar{u}$ is not a function of y at $x = a$ and $\bar{v}$ is not a function of x at $y = b$. Therefore,

$$U = \int_o^\tau \left\{ \left[\int_o^b (N_x)_{x=a} \, dy \right] \left(\frac{\partial \bar{u}}{\partial t} \right)_{x=a} + \left[\int_o^a (N_y)_{y=b} \, dx \right] \left(\frac{\partial \bar{v}}{\partial t} \right)_{y=b} \right\} dt$$

At $t = 0$, $\bar{u}(a,y) = a\alpha T$; $\bar{v}(x,b) = b\alpha T$ and at $t = \tau$, $\bar{u}(a,y) = 0$; $\bar{v}(x,b) = 0$. Therefore, the above energy expression can be written as follows

$$U = -\int_o^{a\alpha T} \left[\int_o^b (N_x)_{x=a} \, dy \right] d(\bar{u})_{x=a} - \int_o^{b\alpha T} \left[\int_o^a (N_y)_{y=b} \, dx \right] d(\bar{v})_{y=b}$$

It is convenient to change the variable of integration to T

$$U = -a\alpha \int_o^T \left[\int_o^b (N_x)_{x=a} \, dy + \frac{b}{a} \int_o^a (N_y)_{y=b} \, dx \right] dT$$

Therefore, if $\partial U/\partial T$ is plotted against the temperature rise T the area under the curve up to the T in question is the recoverable strain energy.

For the third problem (simply supported plate subject to uniform temperature rise with zero displacement of all edges) no terms in the recoverable strain energy disappear. However, at $t = 0$

$$\bar{u}(a,y) = a\alpha T$$

$$\bar{v}(a,y) = y\alpha T$$

$$\bar{u}(x,b) = x\alpha T$$

$$\bar{v}(x,b) = b\alpha T$$

and at $t = \tau$ $u = v = 0$ on all edges, so that, after change of variable

$$U = -a\alpha \int_0^T \left[\int_0^b (N_x)_{x=a}\, dy + \frac{b}{a}\int_0^a (N_y)_{y=b}\, dx + \right.$$

$$\left. \frac{1}{a}\int_0^b (N_{xy})_{x=a}\, y\, dy + \frac{1}{a}\int_0^b (N_{xy})_{y=b}\, x\, dx \right] dT$$

Again, if $\partial U/\partial T$ is plotted against the temperature rise T the area under the curve up to the T in question will be equal to the recoverable strain energy.

Expressions have now been set down for the temperature problems which when plotted will serve as effective load-shortening curves. At buckling the small-deflection theory determines the value of m to use ($n = 1$). Then if curves for other values of m intersect they are also of interest. For the first temperature problem results identical to the compression problem results (see Fig. 1) are obtained except that the abscissa must be changed to

$$\frac{12(1 - \mu^2)}{\pi^2} \frac{b^2}{h^2} \alpha T$$

and P must now be regarded as the edge reaction load. For a discussion of possible changes in buckle pattern see the section entitled "The Phenomenon of Change in Buckle Pattern." It would be expected that changes in buckle pattern would be of the type discussed for the controlled shortening type of loading. Thus the values of m can be taken from Figure 1 for a finite plate, or for the infinite plate the values of $\beta = mb/a$ can be taken from Table 1.

For the second and third temperature problem no intersections occur; thus no changes in buckle pattern are expected from that at initial buckling so that $m = n = 1$. Results are presented for these problems in Figures 14 and 15. In Figure 14 curves are presented for the second problem for plates of length-width ratio 1, 1.5, 2, 4, and ∞. The results for plates of finite length are based on the first and second approximation and the results for infinitely long plates is based on a separate exact solution. It is expected that the curves for finite length-width ratio will become asymptotic to the curve for infinitely long plates. The results for the first and second approximation as plotted in Figure 14 lie reasonably close together for the range of temperature rises shown, and, thus, indicate good convergence for nearly square plates and poorer convergence for higher length-width ratios. Although the results presented here for simply supported plates indicate a pattern of one large buckle for all length-width ratios, it is to be expected that clamped plates with the same in-plane boundary conditions will have more than one buckle for some length-width ratios and may have changes in buckle pattern.

For the third problem the recoverable energy curve is presented in Figure 15 for a square plate along with the corresponding curve for the second problem. Also presented are the infinitely long plate results which were presented in Figure 14. The infinitely long plate results satisfy the boundary conditions for this problem as well as the boundary conditions for the second problem. From the results obtained,

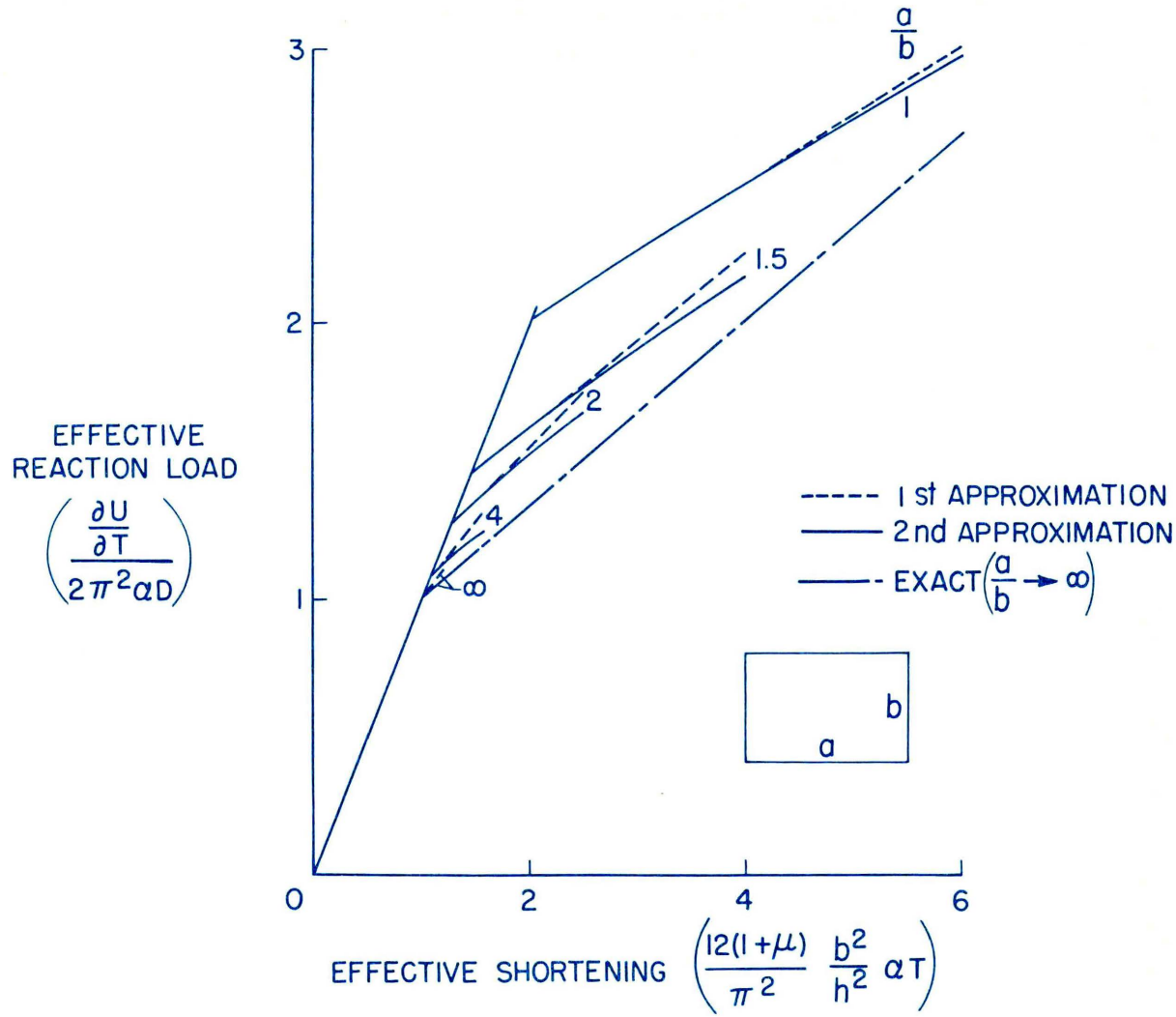

Figure 14.- Effective reaction load-shortening curves for simply supported rectangular plates with zero edge displacement normal to all edges and subjected to a uniform temperature rise.

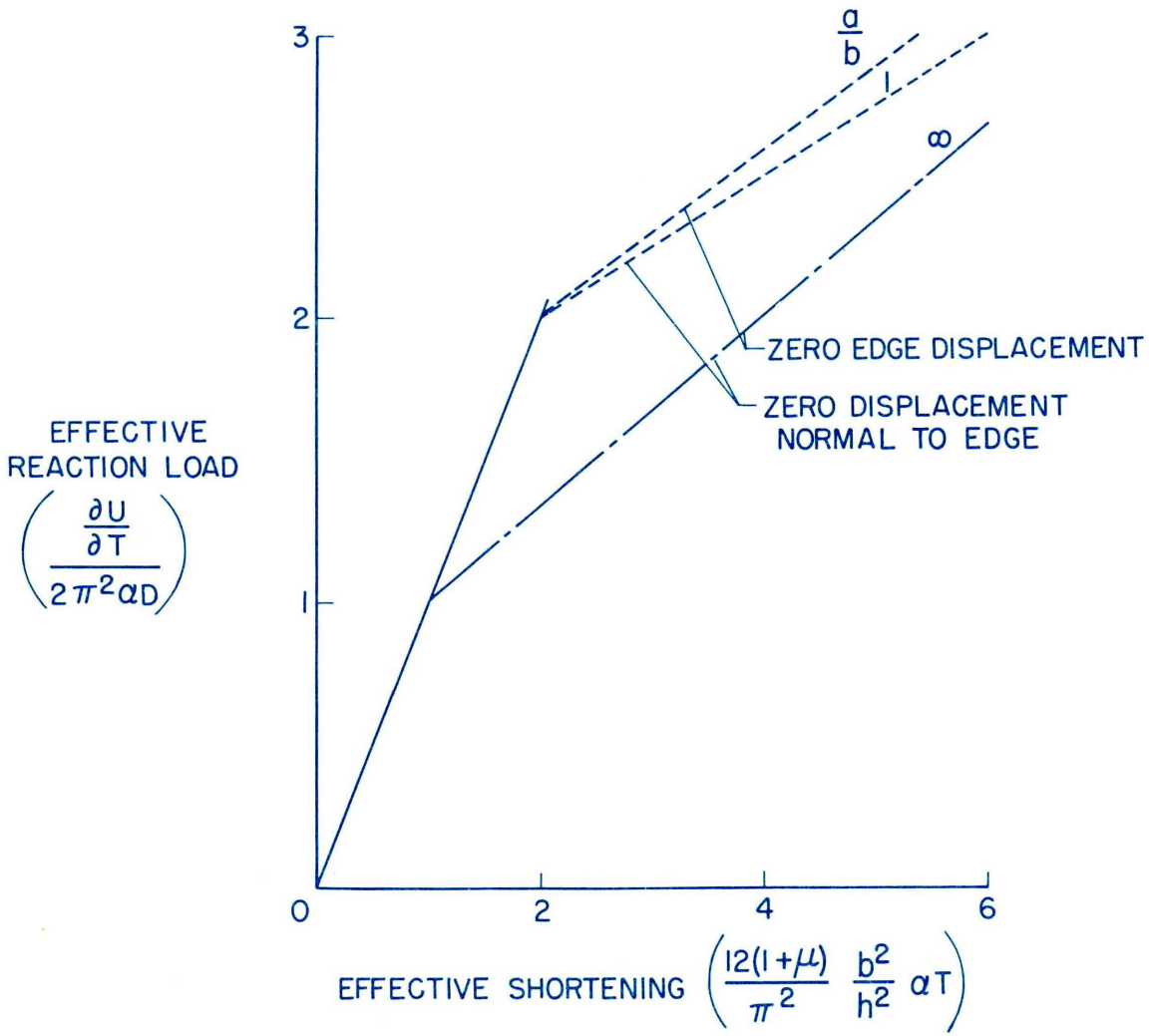

Figure 15.- Comparison of effective reaction load-shortening curves of simply supported plates with various in-plane edge conditions and subjected to a uniform temperature rise.

there is no indication of a change in buckle pattern. Both the square and the infinitely long plate buckle into one large buckle. Again it is to be expected that clamped plates with the same in-plane boundary conditions will have more than one buckle for some length-width ratios and may have changes in buckle pattern. Although Figure 15 indicates somewhat of a difference in recoverable strain energy between the second and third problem for a square plate, a separate calculation shows that the deflection will be essentially the same. However, the stress distributions will be different. For higher temperature rises, the result for finite length-width ratios will become asymptotic to the infinite plate results.

XII. CONCLUDING REMARKS

An advantage of the linear set of equations derived in this dissertation to replace the nonlinear large deflection plate equations is the simplicity of solution. Much more is known about solving linear partial differential equations than about solving nonlinear partial differential equations. An evidence of this simplicity is the worked out solutions presented. However, the linear set of equations are subject to certain limitations for further use according to the application desired. It is to be expected that for certain other problems convergence might be poor, and at the present time it seems that the linear equations cannot be used to solve postbuckling problems for plates with initial eccentricities.

For the compression problem solved, the second approximation of the present theory agrees with exact results for the square plate. Results for plates with finite, as well as infinite, length-width ratio indicate that the effects of change in buckle pattern must be considered. For an infinite plate, results obtained in first approximation agree with the best previous results for much of the range, but results for the second approximation give lower and more accurate loads for given shortenings than previous results.

The comparisons made here indicate that for extreme fiber strains and deflections at the crest of a buckle the present theoretical results for simply supported rectangular plates with straight edges free of shear agree well in the postbuckling range with experimental results on practical stiffened panels.

The analysis of a simple model has been presented indicating the action of change in buckle pattern for two types of loading. The results indicate that intersections between curves for the various equilibrium configurations indicate change in buckle pattern. The load at which change in buckle pattern occurs is shown to be independent of the type of loading, but the manner of change does depend on the type of loading. The change can be continuous or discontinuous, depending on the structure and on the type of loading. Further computations similar to that done for the simple model are necessary to give precisely the secondary buckling load and the transition loading paths for finite rectangular simply supported plates subject to the various types of longitudinal compressive loadings (controlled load, controlled shortening, etc.).

For temperature problems a procedure is developed which permits drawing curves similar to the load-shortening curves of the compression problem for the purposes of indicating possible changes in buckle pattern. Results for the first of the three temperature problems solved is identical except for a few elementary changes to the compression problem and therefore is subject to change in buckle pattern. No buckle pattern change is indicated for the other two problems solved.

XIII. SUMMARY

The nonlinear large deflection plate equations of von Karman are converted into a set of linear equations by expanding the displacements into a power series in terms of an arbitrary parameter. The postbuckling behavior of simply supported rectangular plates subjected to longitudinal compression and subject to a uniform temperature rise is investigated in detail by solving the first few of the equations. By means of a rigorous analysis of a separate model the phenomenon of change in buckle pattern is investigated.

Experimental data are presented for the compression problem. Comparisons are made for total shortening and local strains and deflections which indicate good agreement between experimental results and theoretical results.

XIV. ACKNOWLEDGMENTS

Thanks are due the National Advisory Committee for Aeronautics for permitting this work to be carried out as part of the author's daily work at the NACA Langley Aeronautical Laboratory.

Several members of the staff of the NACA Langley Aeronautical Laboratory and of Virginia Polytechnic Institute are to be cited for having contributed appreciably to this dissertation. Dr. Daniel Frederick of VPI and Dr. J. Lyell Sanders, Jr., of the NACA are to be thanked for their suggestions and encouragement. Particular acknowledgment is due Mr. John M. Hedgepeth of the NACA for his recommendations on the study of change in buckle pattern and for his meticulous review of this dissertation.

XV. BIBLIOGRAPHY

1. von Karman, T.: Festigkeitsprobleme in Maschinenbau. Vol. IV, pt. 4 of Encyk. der Math. Wiss., 1910, art. 27, p. 349.

2. von Karman, Theodor, Sechler, Ernest E., and Donnell, L. H.: The Strength of Thin Plates in Compression. ASME Trans., AMP-54-5, vol. 54, no. 2, Jan. 30, 1932, pp. 53-57.

3. Cox, H. L.: The Buckling of Thin Plates in Compression. R & M No. 1554, British A.R.C., 1933.

4. Timoshenko, S.: Theory of Elastic Stability. McGraw-Hill Book Co., Inc., 1936, pp. 390-395.

5. Marguerre, K., and Tefftz, E.: Uber die Tragfahigkeit eines langsbelasteten Plattenstreifens nach Uberschreiten der Beullast. Z.f.a.M.M., Bd. 17, Heft 2, Apr. 1937, pp. 85-100.

6. Marguerre, Karl: Apparent Width of the Plate in Compression. NACA TM 833, 1937.

7. Kromm, A., and Marguerre, K.: Behavior of a Plate Strip Under Shear and Compressive Stresses Beyond the Buckling Limit. NACA TM 870, 1938.

8. Levy, Samuel: Bending of Rectangular Plates With Large Deflections. NACA Rep. 737, 1942.

9. Koiter, W. T.: De meedragende breedte bij groote overschrijding ker knikspanning voor verschillende inklemming der plaatranden. (The Effective Width of Flat Plates for Various Longitudinal Edge Conditions at Loads Far Beyond the Buckling Load) Rep. S.287, Nationaal Luchtvaartlaboratorium, Amsterdam, Dec. 1943.

10. Hu, Pai C., Lundquist, Eugene E., and Batdorf, S. B.: Effect of Small Deviations From Flatness on Effective Width and Buckling of Plates in Compression. NACA TN 1124, 1946.

11. Coan, J. M.: Large-Deflection Theory for Plates With Small Initial Curvature Loaded in Edge Compression. Jour. Appl. Mech., vol. 18, no. 2, June 1951, pp. 143-151.

12. Mayers, J., and Budiansky, Bernard: Analysis of Behavior of Simply Supported Flat Plates Compressed Beyond the Buckling Load into the Plastic Range. NACA TN 3368, February 1955.

13. Alexeev, S. A.: A Postcritical Study of Flexible Elastic Plates. (In Russian) Prikladnaya Matematika i Mekhanika (U.S.S.R.) vol. XX, no. 6, Nov.-Dec. 1956, pp. 673-679.

14. van der Neut, A.: Post Buckling Behavior of Structures. V.T.R. Report 69, Technical University, Delft, Netherlands, July 1956.

15. Cox, H. L.: The Buckling of a Flat Rectangular Plate Under Axial Compression and Its Behavior After Buckling. R. & M. No. 2041, British A.R.C., May 7, 1945.

16. Ince, E. L.: Ordinary Differential Equations. Longmans, Green and Co., New York, 1927, pp. 213-214.

17. Kotanchik, Joseph N., Weinberger, Robert A., Zender, George W., and Neff, John, Jr.: Compressive Strength of Flat Panels With Z and Hat-Section Stiffeners. NACA Wartime Report L62, 1944.

18. Kotanchik, Joseph N., Zender, George W., and Weinberger, Robert A.: Compressive Strength of Structural Elements for the Northrop XB-35 Airplane. NACA Memorandum Report L5G10a, 1945.

The vita has been removed from the scanned document

POSTBUCKLING BEHAVIOR OF RECTANGULAR PLATES

By

Manuel Stein

ABSTRACT

Unlike simple columns, rectangular plates which are supported on all edges may carry considerable load beyond their buckling load. Under some conditions it may be advantageous to utilize this additional load-carrying capacity. Von Karman has presented the basic nonlinear differential equations for a plate element undergoing large deflections. In this dissertation the nonlinear equations of von Karman are converted into a set of linear equations by expanding the displacements into a power series in terms of an arbitrary parameter. The first few equations of the set can be identified as the usual (linear) small deflection equations. Solution of these and then some of the succeeding equations permits a study of the behavior of the plate at buckling and then beyond into the large deflection range. At present it seems that only plates without initial eccentricities subject to in-plane loading may be solved by the present method. The advantage of the present method is the simplicity of solution.

The elastic postbuckling behavior of simply supported rectangular plates subjected to longitudinal compression and subjected to a uniform temperature rise is investigated in detail by solving the first few of the equations. Results are presented for these problems in the form of equations and curves. Load-shortening curves for the compression problem and similar curves for one of the temperature problems solved indicate that changes in

buckle pattern will occur. Because of the incompleteness and the inconsistancies of the treatment of the phenomenon of change in buckle pattern in the literature, a study of this phenomenon is made. In order to analyze change in buckle pattern in a rigorous fashion the postbuckling behavior of a symmetric three element column on a nonlinear elastic foundation is determined. It is indicated how the principles learned from the column analysis may be applied qualitatively to plate problems.

The results for the plate in compression are compared to previous theoretical results and to experiment. For a square plate the present results agree with previous exact results. For an infinitely long plate the present thesis gives more accurate (lower) loads than previous results. Experimental results which have not been reported previously are described in this thesis, and results from these and other experiment are compared with the present theory. Comparisons are made for total shortening and local strains and deflections which indicate good agreement between experimental results and theoretical results.